2016

Fabrication and Characterization of Buckypapers for Use in Air Sampling

Jonghwa Oh
University of Alabama at Birmingham

FABRICATION AND CHARACTERIZATION OF BUCKYPAPERS FOR USE IN AIR SAMPLING

by

JONGHWA OH

CLAUDIU T. LUNGU, COMMITTEE CHAIR
ANDREI STANISHEVSKY
EVAN L. FLOYD
JULIA M. GOHLKE
MICHELLE V. FANUCCHI
UDAY VAIDYA

A DISSERTATION

Submitted to the graduate faculty of The University of Alabama at Birmingham,
in partial fulfillment of the requirements for the degree of
Doctor of Philosophy

BIRMINNGHAM, ALABAMA

2016

FABRICATION AND CHARACTERIZATION OF BUCKYPAPERS FOR USE IN AIR SAMPLING

JONGHWA OH

ENVIRONMENTAL HEALTH SCIENCES

ABSTRACT

Occupational exposure to volatile organic compounds (VOCs) is a concern from a public health perspective. In many industrial activities, workers' exposure to VOCs can be sufficiently high to induce adverse health effects, so their monitoring is necessary. In exposure assessment, post sampling extraction and quantification are the typical analytical procedures. Recently, our group developed the photothermal desorption (PTD) technique in which a pulse of light thermally desorbs an analyte directly from a sorbent. Advantages of this technique are; it is solvent free, repeated analysis is possible, sorbents are reusable, and no high cost of equipment is required. PTD overcomes almost all drawbacks of current extraction methods. This study was aimed to develop and test a new sorbent which will efficiently work with PTD. Single-walled carbon nanotubes (SWNTs) were examined as potential sorbents because of their high surface area, great thermal conductivity, and efficient light absorption. SWNTs were fabricated into a self-supporting form (i.e., buckypaper (BP)) which will preserve its physical integrity under normal working conditions. Largely two types of SWNTs were used, arc discharge (AD) and high-pressure carbon monoxide (HiPco), and different fabrication methods were

examined. Upon fabrication, their adsorption properties were characterized in terms of Brunauer, Emmett, and Teller (BET) surface area, pore size, and toluene adsorption capacity. HiPco BP and methanol-cleaned AD BP (suspended/rinsed with methanol) were the top two materials, showing the highest surface area (649 and 387 m^2/g, respectively) and adsorption capacity (106 and 46 mg/g, respectively) with relatively small mean pore diameter (7.7 and 8.8 nm, respectively). To further improve the adsorption properties, specific heat treatment conditions for each type of BPs were employed. After initial treatments only HiPco BP and acetone-cleaned AD BP (suspended/rinsed with acetone) were selected for further investigations based on obtained surface area (933 and 970 m^2/g, respectively) and physical integrity. These two BPs were then examined for PTD and the AD BP showed higher recovery rate (0.016 - 0.431 %) at all energy levels examined (1.84 - 7.37 J). The AD BP has been shown to be an efficient sorbent for toluene and possibly a good candidate for PTD.

Keywords: VOC analysis, photothermal desorption (PTD), buckypaper (BP), VOC sorbent, adsorption efficiencies, heat treatment

ACKNOWLEDGEMENTS

I would have never imagined myself coming this far in academia if there were not my endeavor and support from people around me. My advisor, Dr. Lungu, has always been very helpful: he taught me how to logically approach projects and resolve technical issues, always offered to give a hand in my lab work, and was instrumental to my adaptation in the US. I greatly appreciate Dr. Claudiu and Anca Lungu's friendship and their kindness of taking care of me. I cannot think about my research without Evan who taught me everything in the lab from analytical techniques to hodgepodge stuff. It was so grateful to have him as one of my lab colleagues first and later committee members since my doctoral research was the continuation of his work. After his departure he continued to be very involved helping with his ideas and handy lab skills. I also thank the other committee members, Drs. Julia M. Gohlke, Uday Vaidya, Michelle V. Fanucchi, and Andrei Stanishevsky, for their support, advising, and willingness to help me with this project. Their forward thinking of potential applications of this project and further directions were very helpful.

TABLE OF CONTENTS

Page

LIST OF TABLES

Table *Page*

LIST OF FIGURES

Figure *Page*

INTRODUCTION

FABRICATION AND ADSORTPION CHARACTERIZATION OF SINGLE-WALLED CARBON NANOTUBE (SWNT) BUCKYPAPER (BP) FOR USE IN AIR SAMPLERS

HEAT TREATMENT OF BUCKYPAPER (BP) FOR USE IN VOLATILE ORGANIC COMPOUNDS (VOCs) SAMPLING

PHOTOTHERMAL DESORPTION (PTD) OF BUCKYPAPER (BP) FOR USE IN AIR SAMPLERS

INTRODUCTION

Volatile Organic Compounds (VOCs) Sampling and Analysis

Occupational and environmental hazards can be categorized as chemical, physical, biological, and ergonomic. [1] The main route of chemical exposure is through inhalation of gases, vapors, or solids in the form of dusts or fumes. [2] Global atmospheric VOC emissions are estimated as 1300 Tg of carbon per year from nonmethane biogenic and anthropogenic resources. [3] Undoubtedly, industries contribute to a considerable amount of VOC emissions, indicating workers' potential exposure. The general definition of VOCs in the scientific literature is organic chemical compounds whose composition makes it possible for them to evaporate under normal indoor atmospheric conditions of temperature and pressure (20 ˚C and 101325 Pa, National Institute of Standards and Technology (NIST)). [4] Many industries involving spraying, painting, coating, etc. have increased health concerns regarding VOCs exposure in workers. VOCs are known to contribute to a wide variety of acute and chronic health effects; acute effects generally occur rapidly from a short-term exposure whereas chronic effects usually occur as a result of long-term exposure. [5] Common health effects from short term exposure to high levels of VOCs include eye, nose, and throat irritation, nausea, dizziness, worsening of asthma symptoms, etc., while long term exposure to high VOC level can result in liver/kidney damage, central nervous system damage, and cancer. [6-9] A number of

studies reported a higher incidence of myelogenous leukemia among people occupationally exposed to benzene (e.g., preparing adhesives). [10, 11] Benzene can also induce hematotoxicity, aplastic anemia, and lymphoma [12]. Increased incidences of renal-urinary or gastrointestinal defects among offspring of occupationally exposed women (from various occupations) were reported and toluene was suggested as most likely a causative agent. [13] Although most toluene exposure occurs in the workplace, intensive exposure is often found among inhalant abusers, resulting in severe adverse health effects reported. Cerebellar degeneration and cortical atrophy were observed among chronic toluene abusers. [14, 15]

From the public health perspective, which looks to protect the health and well-being of workers, it is necessary to estimate potential exposures and to take measures to minimize or if possible eliminate these exposures. Although there are a number of methods to indirectly assess potential exposures, such as calculating the amount of chemicals used, production rate and output, investigating physical and chemical properties of the used chemicals, etc., the only objective method is to directly measure the amount of contaminants in the workplace environment and possibly in the proximity of each worker.

The assessment of exposure to chemical hazards including VOCs is usually performed through area or personal sampling. In general, area sampling is applied for screening purposes and direct reading instruments (DRIs) are commonly used. Personal sampling is preferred when individual exposure is in question. For a better picture of a worker's exposure through inhalation, personal samplers (i.e., collection devices) are placed close to the breathing zone. The sampling method and collection device or

mechanism for gases or vapors are determined by the characteristics of the contaminant of interest as well as the purpose of exposure assessment, i.e., whether it is for screening or for personal levels of exposure to meet legal compliance requirements.

Sampling methods and mechanisms

In active sampling, a sample train consists of a pump, a sorbent tube, and tubing. A pump is used to pull contaminated air through a sampler (i.e., sorbent tube), which captures the contaminant molecules. Active sampling is effective and well accepted in lower exposure situations due to the relatively high amount of contaminated air collected. However, cost effectiveness and wearer acceptance make this technique unattractive as the pump is both expensive and bulky [16] which can interfere with the movement of workers.

Passive sampling does not involve a pump; it only employs a diffusive badge. This makes passive sampling a more desirable option for both workers and industrial hygienists. The primary advantages of passive sampling are the minimal possibility of technical failure (e.g., calibration, power failure, tubing connection, etc.) and greater wearer acceptance. However, passive sampling is not recommended when there are lower concentrations or sampling occurs over a short duration due to lower sampling rate and consequently lower sensitivity [17].

Absorption and adsorption are the primary sampling mechanisms for air sampling. Gases or vapors completely dissolve in a liquid in the absorption process and bubblers or impingers are the typical collection devices. [18] Newer methods such as sorbent based

sampling have been developed and are replacing these devices. There are still specific conditions (e.g., high humidity) where bubblers and impingers are used. Also bubblers and impingers are recommended by Occupational Safety and Health Administration (OSHA) when dealing with specific analytes. [19] For insoluble or nonreactive gases or vapors, adsorption is commonly employed. [2] Molecules are adsorbed on the surface of a sorbent such as activated charcoal or silica gel packed in a sampling tube through a combination of van der Waals forces, hydrogen bonds, and dipole-dipole interactions. [18] Adsorption following diffusion, a mass transfer by concentration gradient of molecules to the surface of a sorbent (i.e., activated charcoal pad inserted in a passive badge or sampler), is the principal mechanism of passive sampling, often called diffusive sampling. Fick's law describes diffusion, as shown in Equation (1).

$$J = -D\frac{dC}{dx} \tag{1}$$

where J is mass flux ($mg/m^2/sec$); D is the molecular diffusion coefficient (m^2/sec); C is concentration (mg/m^3); x is length or distance (m).

For a gas of known diffusivity and set geometry of the diffusive sampler, effective sampling flow rate can be calculated (Equation 2 derived from Equation 1) and is available from manufacturers of various models of passive samplers; effective sampling flow rate is an order of magnitude lower than flow rates used in active sampling, indicating considerably lower mass collected. [18] Details of the adsorption phenomenon will be discussed in more detail in the next section.

$$Q = \frac{D \times A}{L} \tag{2}$$

where Q is sampling rate (m^3/s); A is cross sectional area of the sampler (m^2); L (or x) is the length of the diffusional path (m).

Adsorption

(Physical) adsorption is defined as the enrichment (positive adsorption) or depletion (negative adsorption) of one or more components in an interfacial layer. [20, 21] Physical adsorption brought by weak solid-gas interaction is easily reversed (i.e., desorption). [22] Temperature and pressure are important factors in the adsorption phenomenon, and they are used to obtain adsorption isotherms in which the amount of adsorbate adsorbed by the material is plotted as the pressure changes at a certain, constant temperature. [22] Among a variety of adsorption models (e.g., Freundlich, Langmuir, Dubinin-Radushkevich, etc.), Brunauer, Emmett and Teller (BET) theory is one of the most widely applied in the gas-solid equilibrium system, assuming multilayer adsorption [23]. Five types of isotherms were originally proposed to characterize a sorbent by Brunauer et al. (i.e., Deming, Deming and Teller), and later IUPAC added a sixth type. [24] Type I is typical of microporous (< 2nm) solids, Type II is macroporous (> 50 nm) or nonporous materials with unrestricted multimolecular adsorption (strong adsorbate-adsorbent interactions), Type III describes weak adsorbate-adsorbent interactions on macroporous or nonporous materials, Type IV shows adsorption of mesoporous (2 – 50 nm) sorbents, Type V is weak adsorbate-adsorbent interactions on mesoporous solids, and Type VI (stepped isotherm) is layer-by-layer adsorption on uniform surface, which is rare. [20, 24, 25] Hysteresis loop in Type IV and V indicates progressive withdrawal of gas

to the system and may appear in other types of isotherms (shown in Figures 1 and 2). The popular theory for the reason behind this phenomenon assumes that mesopores having different filling (adsorption) and empting (desorption) rates by capillary condensation are responsible [26]. Surface area and pore structure (porosity) of sorbents also play an important role in the prediction of adsorption (efficiency), which therefore represent a measure of adsorption [20]. BET theory is commonly used to obtain the surface area of an adsorbent (i.e., BET surface area) based on the amount of adsorbate adsorbed and there are a number of different commercial sorption analyzers commonly used. Some of these machines can also determine porosity and pore size with the assumption of a certain pore shape. Pore size, one of the determinant factors for adsorption efficiency, depends on the characteristics of materials; size can vary widely, even within the same material. Pore filling governs the physical adsorption mechanism in smaller pores or micropores as overlapping the pore wall potentials leads to stronger binding of the adsorbate molecules, enhancing adsorption while larger molecules do not have access to micropores, and no enhanced adsorption takes place. [27, 28] The molecular sieve effect (i.e., size exclusion) can be increased in primary pores (< 0.8 nm) and decreases with increasing pore size. Among VOCs, non-aromatic molecules including methanol, ethanol, isopropyl alcohol, and methyl ethyl ketone have kinetic diameters ranging from 3.8 to 5.3 Å. Kinetic diameters for aromatic molecules including benzene, toluene, xylene range from 5.8 to 6.8 Å. [29]

Analysis of Surface Area and Pore Size

Activated charcoal (SKC Inc. Anasorb CSC, Eighty Four, PA) packed in an active sampler and charcoal pad lined in a passive sampler (3M OVM 3500/3520, Paul, MN) were evaluated with a physisorption analyzer (Micrometirics® ASAP 2020, Norcross, GA) using nitrogen at 77 K. Samples were degassed for 1 hour at 300 ˚C prior to analysis. Figures 1 and 2 show the isotherms and Table 1shows the measured adsorption characteristics obtained from the isotherms. Both sorbents indicated the same Type I isotherm with a shallow hysteresis loop and showed high BET surface area with small mean pore diameter (1.7 nm for both). Activated charcoal had a higher BET surface area (1233 m^2/g) but smaller micropore proportions. This preliminary analysis indicated that the commercially available VOC sorbents have great adsorption properties.

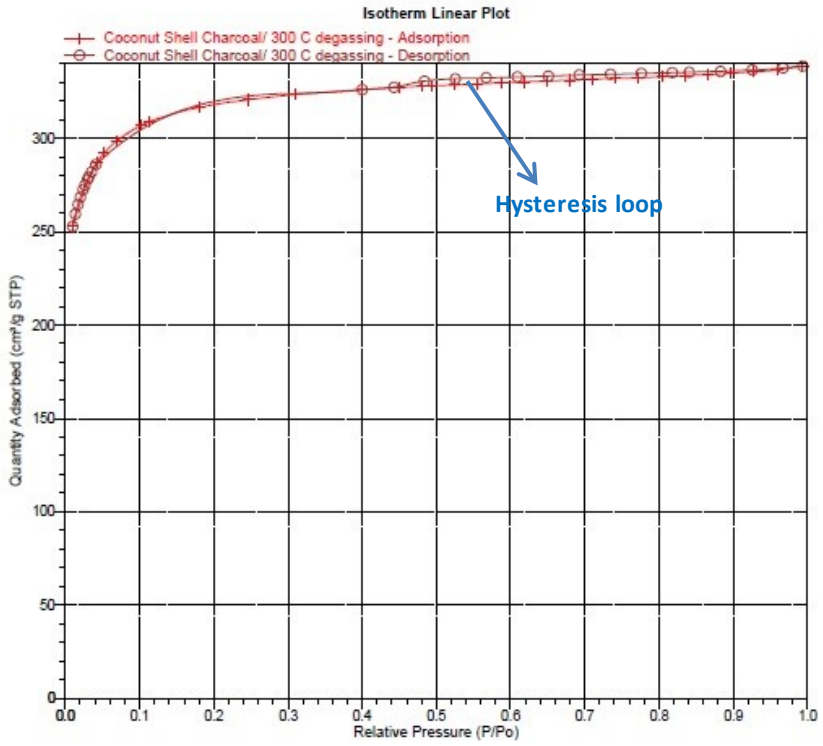

Figure 1. Adsorption and Desorption Isotherms on Coconut Shell Charcoal

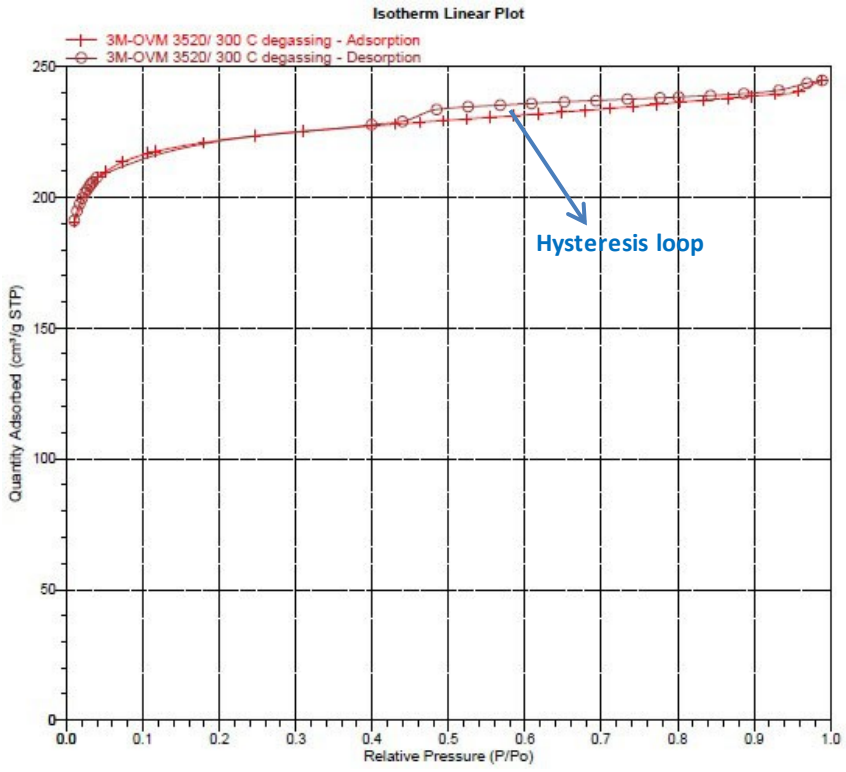

Figure 2. Adsorption and Desorption Isotherms on Charcoal Pad

Table 1. Adsorption Characterization of Commercially Available Organic Vapor Sorbent

	BET surface area (m^2/g)	Micropore area (%)	Pore volume (cm^3/g)	Micropore volume (%)	Mean pore size (nm)
Activated charcoal[1]	1233	82	0.5241	75	1.7
Charcoal pad[2]	879	88	0.3785	78	1.7

[1] Sorbent packed in commercially available active samplers for primarily nonpolar organic compounds

[2] Sorbent substrate lined in passive sampling badges for organic compounds

VOC Analysis

Once VOCs are adsorbed on the sorbent surface of either active or passive samplers, the analytes are usually desorbed through chemical or thermal desorption prior to gas chromatography (GC) analysis. Chemical desorption is the preferred method recommended by National Institute for Occupational Safety and Health (NIOSH) while thermal desorption is a good alternative recommended by Environmental Protection Agency (EPA). [30-35] The EPA method is more appropriate for environmental sampling which commonly deals with lower concentrations, requiring enhanced sensitivity for analysis.

Chemical desorption (or solvent extraction) of contaminants adsorbed on activated charcoal is the most common analytical procedure for occupational VOC exposure evaluation, usually using carbon disulfide. [30] The manual extraction process [36], toxicity of carbon disulfide [37], and low sensitivity due to a small amount injected into GC are often noted as disadvantages of this method.

Thermal desorption eliminates solvent use and was traditionally one shot analysis, enhancing sensitivity which is useful when lower exposure level is expected. [38] Recent developments in this technique allows for repeated analysis by re-collecting split flows. [39, 40] Porous polymer sorbents such as Tenax® or Chromosorbs® and carbonaceous sorbents such as Carbopack™ can be used. [35] The selection of sorbents is based on the volatility of the analyte and other factors such as hydrophobicity and thermal stability. This technique requires an expensive desorption unit [30] and system integrity checks (e.g., leak tests) recommended whenever used [35].

Advanced extraction techniques have been developed and tested. [30, 41, 42] Fabrizi et al. used a commercially available accelerated solvent extraction (ASE) system for 57 VOCs desorbed from activated charcoal, using organic solvents such as acetonitrile, acetone, ethyl acetate, ethanol, isopropanol, methanol, and n-hexane through automated extraction under elevated temperature and pressure. [30] 44 VOCs showed a mean recovery of over 96 %. Acetone was the most promising solvent to replace carbon disulfide. Alternative solvent use, short extraction time, and minimal sample preparation were all noted as benefits. [30] Conversely, the high initial expense for the equipment and extract clean-up have been noted as disadvantages. [41] Solid phase microextraction (SPME) allows for a single step of sampling and pre-concentration and then direct transfer of analytes into GC. [43] Koziel et al. tested a SPME system in which silica fiber coated with extracting polymer (a variety of available coatings) and housed in a needle was used to sample VOCs which were desorbed (thermally with injector heat) by injecting the needle into GC where the fiber was exposed to carrier gas. [42] VOC concentrations of benzene, toluene, ethylbenzene, xylene, and hexane were comparable with concentrations obtained through the standard NIOSH method. SPME has been suggested to be fast, sensitive, and cost-effective (re-usable sampler & no thermal desorption unit). [42] Some drawbacks are slow partition equilibrium for low volatile analytes, temperature correction for equilibrium composition, and poor storage stability. [43] Recently, our group has developed an alternative desorption technique called photothermal desorption (PTD) which is described further.

Photothermal Desorption (PTD) [44, 45]

Phtotothermal desorption (PTD) is a new pre-analysis technique with enhanced sensitivity for the detection of low mass, especially that which is collected on a passive sampler. PTD is a technique with minimal initial investment for equipment and it allows repeated analysis. Given PTD's ability to fill the gap between chemical and thermal desorption and other benefits noted above, it should be a welcome innovation in the occupational/environmental exposure assessment fields. With PTD, there is no sample preparation (faster analysis), use of toxic solvents, or costly equipment necessary, and it provides greater sensitivity than chemical desorption. Analysis can be repeated and the sorbent could be reused after oven desorption treatment. Not only is this technique cost-effective, but also due to the reuse of the sorbent, PTD is environmentally friendly. In PTD, a pulse of light thermally desorbs an analyte collected on a sorbent substrate and analytical equipment such as a photoionization detector (PID) or GC is used for speciation and/or quantitative analysis. However, we are still in the process of identifying the most efficient sorbent for PTD. In our previous studies, chemical vapor deposition (CVD) single-walled carbon nanotubes (SWNTs) were tested as a potential sorbent due to their high surface area, excellent thermal conductivity, and efficient light absorption (this will be discussed in detail later). 50 mg of SWNT powder (+ 90 % pure, MKnano, Ontrio, Canada) were preloaded with 435 μg toluene (Fisher Scientific Certified ACS, Pittsburgh, PA) vapor and desorbed with a 12-V DC, 50-W incandescent/halogen lamp for 4 minutes in a 75 mL dynamic system connected to a PID and compared with activated charcoal (SKC Inc. Anasorb CSC, Eighty Four, PA). Mean desorption percentage of SWNTs was 72.6 %, higher than activated charcoal (45.8 %). In the

following study, SWNT felt was fabricated by suspending 20 mg SWNTs in 150 mL toluene, sonicating for approximately 30 minutes, and then depositing them onto a silver membrane filter under vacuum (vacuum filtration method). Three types of samples including SWNT powder (SWNT-p), activated charcoal powder (AC-p, Sigma-Aldrich Co., St. Louis, MO), and SWNT felt (SWNT-f) were preloaded with 435 μg toluene vapor and desorbed at four light energies (0.77 – 4.77 J) with a photographic grade xenon flash lamp (NEEWER® 250DI, Neewer Technology ltd., Guangdong, China). A total of ten flashes were delivered to a sample chamber with a glass window to allow the light penetration. Desorption was determined for one flash and ten flashes. Desorption was significantly higher for SWNT-f compared with AC-p and SWNT-p at all flash energies. With a single flash, using SWNT-f, the desorbed mass ranged from 0.25 to 3.76 μg (0.057 – 0.864 %) and with ten flashes, desorbed mass ranged from 1.79 to 33.53 μg (0.411 – 7.708 %).

Carbon Nanotubes (CNTs)

The first notable discovery of CNTs was by Iijima in 1991, which were multi-walled carbon nanotubes (MWNTs) by arc discharge (AD) methods. [46, 47] CNTs can be largely categorized into single-walled carbon nanotubes (SWNTs) and multi-walled carbon nanotubes (MWNTs). SWNTs are formed by rolling a graphene sheet into a cylinder along an (m,n) lattice vector which determines the diameter and chirality [48] while MWNTs are multiple layers of graphene sheets [49]. Depending on the diameter and chirality, CNTs can be either metallic or semiconducting, and a high aspect ratio is

characterized with small diameter (typically 1 nm for SWNTs [50]) and long length (up to many micrometers). [51]

CNTs are well known for excellent thermal conductivity, high surface area, strong mechanical properties, efficient light absorption, etc. [51-53], and further treatment procedures can improve their performance depending on the area of application. For applications in electronics and thermal management [54], examining thermal conductivity of CNTs is important. Experimental measurements have reported exceptionally high thermal conductivity of MWNTs (1400 to 3000 W/m·K) and for SWNTs the values were even higher. [55] A SWNT (2.6 μm in length with 1.7 nm in diameter) was measured to have thermal conductivity as nearly 3500 W/m·K (at room temperature) [54] and a SWNT having a length of 41 μm with a diameter of 1.8 nm showed 2400 W/m·K [56].

Although the high surface area of CNTs has been generally accepted in the literature, it is found to have a broad range. Surface area of arc discharge (AD) SWNTs was 376 m^2/g which increased to 429 and 483 m^2/g after HNO_3 and HCl treatment, respectively. [57] The raw material showed Type IV isotherm while the treated materials (i.e., after acid treatment) were Type II. Average diameter was estimated as 1.1 nm for all the samples and the HCl treated sample developed another peak at 1.3 nm, possibly due to the elimination of some graphitic layers near opened tip. Chemical vapor deposition (CVD) CNTs consisting of SWNTs and MWNTs obtained a surface area of 790 m^2/g after HCl treatment and a pore diameter in the range of 0.8 – 5 nm which was observed through electron microscopy [58]. 524 m^2/g surface area (3.5 nm average pore diameter) was measured with high-pressure carbon monoxide (HiPco) SWNTs and by using two step purification with HCl-washing after air oxidation, surface area increased to 861 m^2/g

(1.0 nm average pore diameter).[26] Adsorption isotherm changed from Type II to Type IV after the purification, suggesting the development of mesopores. However the purified sample's surface area was greatly improved by a marked increase in micropore volume. In another study, surface area and mean pore diameter of HiPco SWNTs were measured as 567 m^2/g and 7.4 nm, respectively. [59] Through a two-step purification process (debundling and HCl treatment/wet oxidation), surface area increased to 1587 m^2/g and pore diameter decreased to 3.9 nm. All isotherms were Type IV and pores were evenly distributed throughout the pore size range, but pores of diameter > 30 nm rapidly decreased after the purification.

CNTs with different synthesis methods (precursor, catalyst, pressure, temperature, etc.), different degrees of purity levels, and different pretreatment methods (acid digestion, heat treatment, etc.) prior to analysis contribute to the somewhat broad range of surface area and pore structure. Depending on the synthesis method, CNTs can be generally categorized into chemical vapor desorption (CVD), high-pressure carbon monoxide (HiPco), arc discharge (AD), and laser ablation. [48] We will briefly introduce the three methods used in our study, CVD, HiPco, and AD in the following section.

Chemical vapor desorption (CVD) [47, 60] emerged as a large scale production in which hydrocarbon gas (e.g., ethylene, methane or acetylene) is decomposed to produce CNTs at 600 – 900 ˚C to yield MWNTs. A higher temperature (900 – 1200 ˚C) is employed for SWNTs. CNTs grow on metal catalysts (e.g., Fe, Co or Ni) above the substrate (e.g., silica, quarts or zeolite) and CNT diameter is closed related to the metal catalyst. In the high-pressure carbon monoxide (HiPco) [47, 61] process developed at Rice University in 1999, iron catalysts such as iron pentacarbonyl ($Fe(CO)_5$) are decomposed

in CO flow under higher pressure (30 – 50 atm) and at a temperature ranging from 900 – 1100 ˚C to produce SWNTs only. Due to simultaneous reaction and free substrates, large scale synthesis is possible. Arc discharge (AD) [47, 60] method is one of the oldest methods found by Iijima in which carbon nanotubes are produced by the sublimation of graphite through a high temperature arc (> 3000 ˚C) generated by DC power between two electrodes. Generally, the anode is either a pure graphite rod or a graphite rod with catalyst added (e.g., Fe, Ni, Co, etc.) and the cathode where CNTs are deposited is pure graphite. Without the metal catalyst MWNTs are the most abundant. Energy intensive and large scale process can be limited by use of solid carbon precursor to be evaporated.

Theoretical analysis has predicted exceptionally high mechanical properties of CNTs, a promising strong and light-weight material, having approximately 100 times more strength than general metals [62, 63], although experimental data have demonstrated mechanical properties to be lower than the estimates. A variety of factors play a role on the measurement of mechanical properties, resulting in a somewhat wide range of values which are still comparable between studies. The tensile strength of laser ablation SWNT ropes was measured to be 45 ± 7 GPa. [64] Aligned CVD SWNT ropes showed tensile strength as high as 22 ± 2 GPa. [65] Average tensile strength of aligned CVD MWNTs was much lower as 1.7 ± 0.6 GPa and Young's modulus (E) was 0.45 ± 0.23 TPa. [66] E of outmost layer of AD MWNTs were measured in a range from 0.25 to 0.95 TPa. [67] Laser ablation 27 SWNTs yielded E of 1.25 TPa as an average. [68] Measurement of mechanical properties of individual SWNT is often challenged by their small diameter and bundling effect. [68]

A black body is a theoretical system that absorbs all incoming radiation [69], and has a great implication for applications in thermal sensors [70], solar energy collectors [71], etc. as it efficiently converts light to heat [53]. A forest of vertically aligned SWNTs showed behaviors similar to a black body, absorbing light at a very wide spectral range of 0.2 to 200 μm. [53] Vertically aligned CVD MWNTs also showed great absorption in the visible and near infrared regions. [72] Increased light absorption was observed with a CNT layer coated on $Bi_2Sr_2Co_2O_y$ thin films examined for light-induced transverse thermoelectric effect. [73]

Due to the unusual properties noted above, CNTs have been used extensively in a wide variety of applications including biomedicine, electronics, energy, etc. [52, 74] The adsorption mechanism is one of the especially promising applications, mainly for energy storage purposes (e.g., H_2, CH_4, Ar, Xe, Kr, etc.) [75-79]. For closed-end SWNT bundles, three possible adsorption sites include the interstitial channels (IC) between the nanotubes, the grooves of two adjacent outer nanotubes (G), and the convex outer surface (S) [80, 81], as shown in Figure 3. So far, studies have been conflicted regarding the adsorption of molecules on the IC. [75, 82, 83] There is also controversy over which molecules can be adsorbed on the IC. He [84] and Kr [78] have been addressed to be adsorbed on the IC while CH_4's adsorption is under debate [78, 83]. There is no universal agreement or explanation for this phenomenon but the size of molecules and their interaction energy may contribute to this complicated nature [82]. Interstitial defects by heterogeneous bundles, allowing the adsorption of gases, have also been also addressed as possible causes. [75, 85]

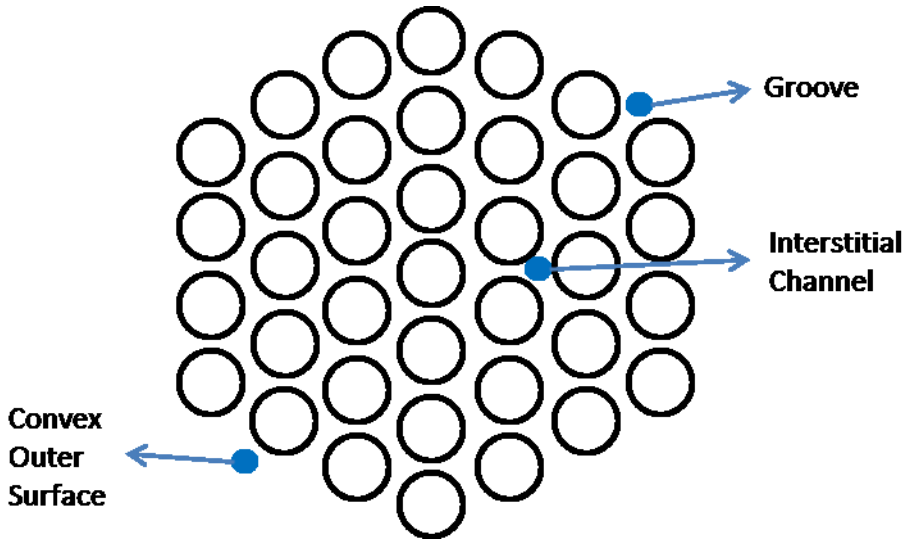

Figure 3. Possible Adsorption Sites of Closed-end SWNT Bundle

As-produced SWNTs generally have closed ends. [80] Cap openings, cuttings, and defects can happen when a harsh purification process is utilized (e.g., acid treatment, refluxing, etc.). [86] In such cases, adsorption can also occur inside the tubes, increasing adsorption capacity. Mechanically cut AD SWNTs were tested for Kr and Xe adsorption and it was concluded that some of the IC were available to those molecules. [87] In a following study, carbon tetrachloride (CCl_4) was examined and evidence for IC adsorption was found on AD SWNTs. [80]

Buckypaper (BP) Sorbent

In our previous studies, we were unable to fabricate SWNTs into a structurally rigorous, self-supporting form of CNTs (i.e., buckypaper (BP)). BP or CNT films would be of benefit when used as a substrate in passive samplers as well as other applications (e.g., sensor or filter). Many strategies to fabricate BP or CNT films have been reported

and wet process approaches such as vacuum filtration, solution spraying, layer-by-layer assembly, and spin coating have been widely used. [88, 89] Due to the relatively inexpensive initial cost and the easy procedure (technique), a vacuum filtration method was employed for this study. In this technique, CNTs suspended in solvent are filtered under vacuum, and then CNT cake deposited onto a membrane filter is delaminated to make a BP. Two types of SWNTs (AD and HiPco) were investigated to obtain a BP and subsequently, to compare adsorption and desorption characteristics between materials.

The purpose of this study was to develop a new sorbent with which the PTD technique could be efficiently used. In the first study, fabrication methods of AD and HiPco SWNTs into BPs were examined. Their adsorption properties were characterized in terms of surface area, pore size, and adsorption capacity. Toluene was used as a representative VOC in alignment with our previous studies, other comparable studies, and its similarity to benzene (carcinogen) [44, 90-92]. The physical integrity of the fabricated BPs was additionally investigated because of the importance of their physical stability. In order to successfully use BPs as a substrate in passive samplers, they must be reusable and durable, i.e., retaining physical integrity under normal sampling/working conditions. In the second study, the effect of heat treatment on adsorption characteristics of BPs was investigated to improve their adsorption properties. Heat treatment conditions were designed by the type of SWNTs based on thermogravimetric analysis (TGA) to find the condition which yielded the most desirable adsorption properties. In the third study, PTD was examined with heat treated BPs selected from the previous studies based on their adsorption properties. A Photographic grade xenon lamp was used as a light source and

desorption was determined using PID data. A single pulse of light was used at different energy levels and desorption between the fabricated BP types was compared.

The three papers presented further will clarify some of the aspects of fabricating and selecting sorbents which will make this technique feasible and effective.

FABRICATION AND ADSORPTION CHARACTERIZATION OF SINGLE-WALLED CARBON NANOTUBE (SWNT) BUCKYPAPER (BP) FOR USE IN AIR SAMPLERS

by

JONGHWA OH, EVAN L. FLOYD, TYLOR C. WATSON, CLAUDIU T. LUNGU

Anal. Methods. 2016, 8, 4197-4203

Format adapted and errata corrected for dissertation

ABSTRACT

Single-walled carbon nanotubes (SWNTs) have been investigated as a promising sorbent for volatile organic compound (VOC) sampling. We also successfully demonstrated that pre-analysis desorption can be achieved by irradiating the sorbent with high intensity visible light pulses. This technique, photothermal desorption (PTD), can improve sensitivity and shorten current analytical procedure. Different fabrication methods of a buckypaper (BP), a self-supporting form of carbon nanotubes (CNTs), were explored; three methods using arc discharge (AD) SWNT included non-cleaned, acetone-cleaned, and methanol-cleaned and one method using high-pressure carbon monoxide (HiPco) SWNT. Adsorption efficiencies of the fabricated BPs were compared in terms of Brunauer, Emmett, and Teller (BET) surface area, pore size, and toluene adsorption capacity. All materials were found to have high BET surface area (211 to 649 m^2/g) and toluene adsorption capacity (25 to 106 mg/g) but HiPco BP exhibited the highest BET surface area (649 ± 3 m^2/g) with the smallest mean pore size (7.7 ± 0.3 nm) and the greatest toluene adsorption capacity (106 mg/g). Additionally, HiPco BP had the simplest fabrication process which taken as a whole is clear indication that further investigations using the PTD technique should be explored with this material.

INTORDUCTION

Passive sampling of volatile organic compounds (VOCs) followed by laboratory analysis either through chemical or thermal extraction has been accepted in the workplace because of the convenience, cost effectiveness, and wearer acceptability of passive samplers over active sampling devices. [1-3] However, passive samplers are generally limited in capability for very low exposure situations or short duration sampling because of their higher limit of detection caused by the relatively slow sampling rate driven by diffusion. [4] Moreover, for industries seeking to demonstrate regulatory compliance, the long time lag between collecting samples and getting results back [5] and expensive laboratory analysis have been a burden. Recently, our group developed a novel analytical technique called photothermal desorption (PTD) which can improve the sensitivity of the analysis of passive samplers and help shorten the current exposure assessment procedure to improve workers' protection by faster turn-around-time for analytical results. [6] In PTD, a pulse of light thermally desorbs analyte collected on a sorbent which releases VOC. VOC can be directly measured with a photo-ionization detector (PID) or directed to a gas chromatograph (GC) for detailed analysis. However, further development of a new sorbent which will work efficiently with this new desorption technique is still needed.

In this study, single-walled carbon nanotubes (SWNTs) were evaluated as potential sorbents for PTD because of their efficient light absorption [7, 8], exceptionally high thermal conductivity [9, 10], and high Brunauer, Emmett, and Teller (BET) specific

surface area [11]. While in general carbon nanotubes (CNTs) have shown promising features for VOC adsorption [12-14], for passive sampling applications they need to be fabricated into a reusable, sturdy form which will preserve its physical integrity under normal working conditions. The purpose of this study was to examine fabrication methods of SWNTs to obtain BPs that are favorable for use with PTD. To accomplish this we compared their adsorption properties through examining BET surface area, average pore size, and toluene adsorption capacity. Previously, SWNTs synthesized by chemical vapor deposition (CVD) were examined due to their low cost and the scalability of synthesis. [6] However, we were unsuccessful in processing CVD SWNT into a self-supporting form (i.e., buckypaper, BP). Therefore, in this study SWNTs obtained through arc discharge (AD) and high-pressure carbon monoxide (HiPco) syntheses were investigated since we were able to easily process these into BPs in our lab. Additionally, mechanical properties of the fabricated BPs were characterized to examine their physical integrity.

EXPERIMENTAL

Fabrication of Buckypapers (BPs)

High purity AD SWNT and HiPco SWNT were purchased from NanoIntegris Inc. (Quebec, Canada). AD SWNT (94.5 %) was pre-suspended in a surfactant solution (0.5 mg/mL, 1 % w/v sodium cholate and 1 % w/v sodium dodecyl sulfate in water). HiPco SWNT was powder (85 %). Vacuum filtration of liquid suspended SWNT was employed to fabricate BPs [15, 16] with a cleaning process added to remove potential surfactants from

the AD SWNTs based on the manufacturer's recommendations [17]. For the fabrication of AD BPs, 100 mL (50 mg) of the AD SWNT suspension was mixed with 400 mL of acetone for 15 hours (Figure 1). The suspension was then vacuum-filtered through a polytetrafluoroethylene (PTFE) membrane filter (47 mm diameter, 5 μm pore, EMD Millipore, Darmstadt, Germany) and allowed to dry for 30 minutes under vacuum and another 2 hours without vacuum while on the filter membrane. A BP was obtained by delaminating the dried SWNT cake from the filter (non-cleaned AD BP). For solvent cleaned BPs, a series of two alternating rinses were used, a water rinse then solvent rinse was administered after the SWNT cake was deposited but not dried. The SWNT cake was first rinsed with 250 mL of deionized water (18.2 MΩ-cm) then 50 mL of solvent to make either acetone-cleaned or methanol-cleaned AD BP.

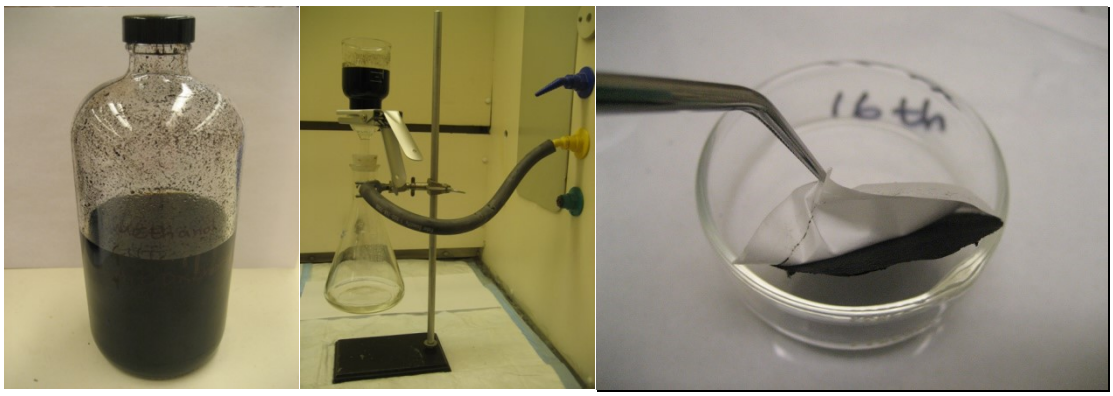

Figure 1. Typical Fabrication Procedure: CNT Suspension - Vacuum Filtration - Delamination (left to right)

For HiPco BP preparation, 50 mg of powdered HiPco SWNTs were suspended in 400 mL methanol and ultra-sonicated using a 490 W bath sonicator (BRANSON CPX5800H, Danbury, CT) for 90 minutes. The solution was vacuum-filtered through the

same type PTFE membrane filter and allowed to dry for 30 minutes under vacuum plus another 2 hours without vacuum. The SWNT cake was then delaminated from the filter to obtain a BP (HiPco BP). Four BPs per each fabrication method were produced and each BP was investigated according to the diagram shown in Figure 2.

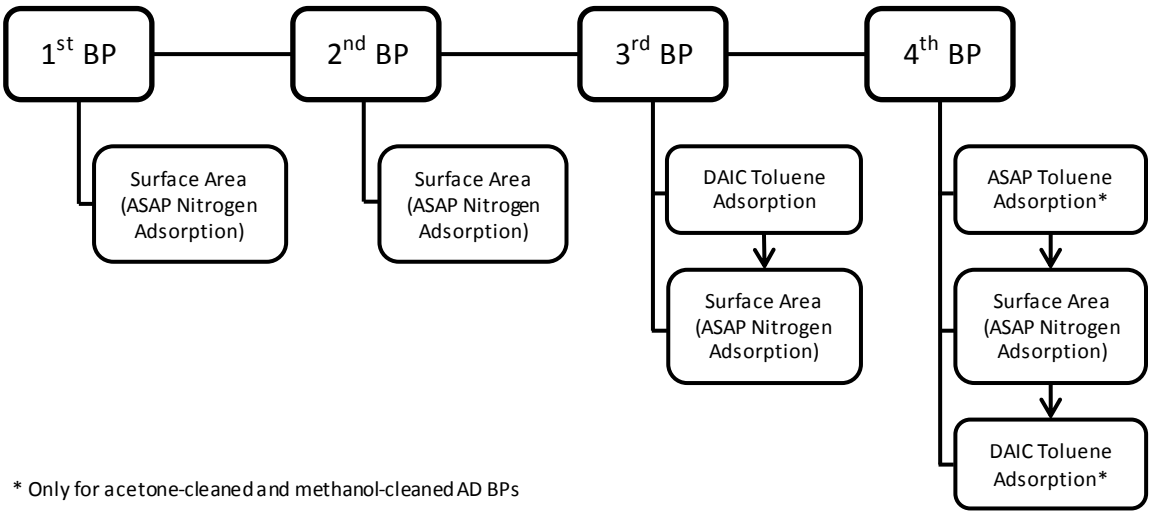

Figure 2. Diagram of Measurements Assigned to BPs of Each Fabrication Method

Adsorption Characterization of BP

Three adsorption parameters were examined: BET surface area, average pore width, and toluene adsorption capacity. A physisorption analyzer (Micromeritics® ASAP 2020, Norcross, GA) was used to obtain surface area and average pore width by N_2 physisorption at 77 K. Samples were desorbed at 100 ˚C overnight in a lab oven prior to any adsorption parameter measurements. Degassing was conducted with the physisorption analyzer for 60 minutes at 300 ˚C to further remove impurities prior to

analysis. Nitrogen adsorption isotherms were used to determine surface area by BET theory. The average pore width was determined by;

$$d = \frac{4 \times V}{A} \times 10^3 \quad (1)$$

where d is average pore width (nm), assuming cylindrical pores; V is single point total pore volume (cm^3/g) at relative pressure ≥ 0.995; A is surface area per unit mass of a sorbent determined by BET theory (m^2/g).

Three BPs per fabrication method were analyzed by N_2 physisorption (Figure 2) with each sample analyzed in triplicate and results averaged.

A diffusive based VOC adsorption isotherm chamber (DAIC) was designed in our lab to obtain toluene adsorption isotherms (30 ˚C, 303.15 K) and determine adsorption capacity at a given equilibrium concentration (Figure 3). Toluene flux into the DAIC system was first characterized with a toluene diffusion tube connected to an empty chamber. Toluene concentration in the chamber was continuously monitored with an

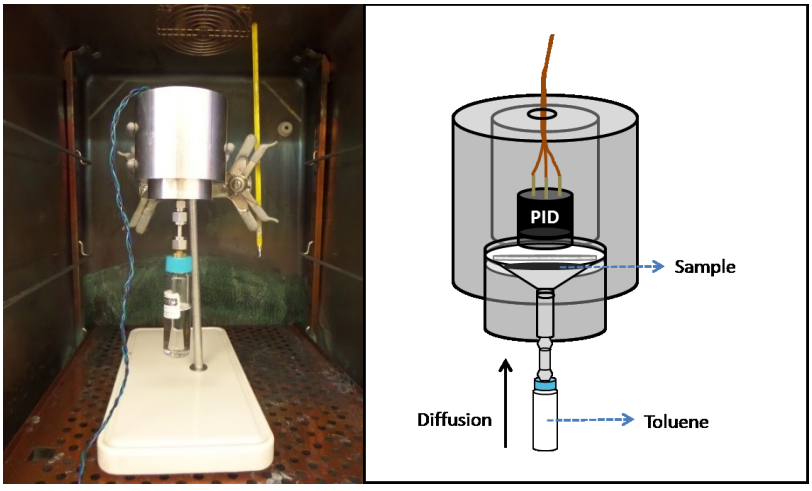

Figure 3. Diffusive Adsorption Isotherm Chamber (DAIC) System (picture and detailed diagram)

photo-ionization detector (PID, VOC-TRAQ, Baseline®, Lyons, CO). The mass flux of the toluene was determined by measuring the mass change in time as shown in Equations (2) and (3);

$$F = \sum_{i=1} \frac{\Delta m}{\Delta t} \tag{2}$$

where F is mass flux of the adsorbate (μg/s); Δm is mass change of adsorbate in the chamber across the time interval (μg); Δt is time interval between measurements (i.e., logging time interval of PID) (s).

$$\Delta m = \left(\frac{\Delta C}{V_m} \times MW \right) \times V_C \times 10^3 \tag{3}$$

where ΔC is concentration change of the adsorbate in the chamber during the time interval as measured with the embedded PID (ppm); V_m is 25.04, molar volume at the analytical temperature (303.15 K) and pressure (98992 Pa); MW is molecular weight of adsorbate (92.14 g/mol for toluene); V_C, is volume of the chamber (47.3 x 10^{-6} m^3).

The characterization measurements were repeated 6 times and a linear regression equation performed on all 6 trials to obtain an averaged adsorbate mass flux (R^2 = 0.85) that accounted for the dynamic concentration gradient as the isotherm progressed;

$$F = \{-0.000158 \times (C_{eq})\} + 0.185214 \tag{4}$$

where F is mass flux of the adsorbate (μg/s); C_{eq} is equilibrium concentration (ppm).

The mass adsorbed by a sorbent in a given isotherm was calculated using Equation (4) from the concentration in the DAIC over time. Adsorption was allowed to proceed until equilibrium concentration exceeded 800 ppm toluene. Adsorption capacity was expressed as mg (toluene)/g (sorbent).

The third BP from each fabrication method (Figure 2) was also analyzed for its toluene adsorption capacity using the DAIC system prior to surface area measurement.

To validate the DAIC system, activated carbon sorbent was placed in the DAIC and adsorption allowed to proceed for 2 – 18.5 hours with gravimetric confirmation of actual mass adsorbed at 5 time intervals (2, 2.3, 4, 5, 18.5 hours). The mean prediction was 87.7 ± 12.3 % of actual mass. Additionally two samples (one acetone-cleaned and one methanol-cleaned AD BPs) were sent to Micromeritics® for toluene adsorption analysis by ASAP 2020 physisorption analyzer. Samples were degassed for 960 minutes at 300 ˚C before analysis and analysis was repeated. Adsorption capacity was calculated by converting the adsorbate gas volume at STP (averaged data obtained from the physisorption analyses) to toluene mass using;

$$m_{adsorbed} = \frac{V_{Gas \cdot STP} \times P_{STP} \times MW \times 10^3}{R \times T_{STP}} \quad (5)$$

where $m_{adsorbed}$ is mass adsorbed per gram of sorbent (mg/g); $V_{Gas \cdot STP}$ is gas volume at STP obtained from the physisorption analysis (cm^3/g); P_{STP} is standard pressure (101,325 Pa); MW is molecular weight of toluene (92.14 g/mol); R is ideal gas constant (8.314 $Pa \cdot m^3/mol \cdot K$); T_{STP} is standard temperature (273.15 K).

After the samples were returned, toluene adsorption and BET surface area were re-analyzed since Micromeritics® conducted a substantially longer degassing time (300 ˚C, 960 minutes) than was used in our lab (300 ˚C, 60 minutes).

Mechanical Properties of BP

The mechanical properties of the methanol-cleaned AD BP and HiPco BP were examined through dynamic mechanical analyzer (TA Instruments RSA-G2, New Castle, DE). For the test 25 mg of each material were used to fabricate BPs. Tensile strength and Young's modulus (E) were determined from the stress-strain curve obtained through the analyzer.

RESULTS AND DISCUSSION

BET Surface Area & Pore Size

The BET surface area and mean pore diameter are as follows for non-cleaned AD, acetone-cleaned AD, methanol-cleaned AD, and HiPco BPs; 211 ± 61 m^2/g (8.2 ± 0.1 nm), 322 ± 38 m^2/g (9.7 ± 0.5 nm), 387 ± 16 m^2/g (8.8 ± 0.4 nm), and 649 ± 3 m^2/g (7.7 ± 0.3 nm), respectively (Table 1). After degassing for 960 minutes at 300 ˚C, BET surface area and mean pore diameter were as follows; 205 ± 1 m^2/g (9.7 ± 0.1 nm), 349 ± 10 m^2/g (9.8 ± 0.1 nm), 421 ± 6 m^2/g (8.6 ± 0.1 nm), and 611 ± 56 m^2/g (7.3 ± 0.3 nm) for non-cleaned AD, acetone-cleaned AD, methanol-cleaned AD, and HiPco BPs, respectively.

Table 1. Surface Area (SA) and Mean Pore Diameter (d) Analysis

	Standard degassing (60 min, 300 ˚C)		Extended degassing (960 min, 300 ˚C)	
Fabrication methods	BET SA (m^2/g)	d (nm)	BET SA (m^2/g)	d (nm)
Non-cleaned AD BP	211 ± 61	8.2 ± 0.1	205 ± 1	9.7 ± 0.1
Acetone-cleaned AD BP	322 ± 38	9.7 ± 0.5	349 ± 10	9.8 ± 0.1
Methanol-cleaned AD BP	387 ± 16	8.8 ± 0.4	421 ± 6	8.6 ± 0.1
HiPco BP	649 ± 3	7.7 ± 0.3	611 ± 56	7.3 ± 0.3

In general, adsorption capacity is considered to be proportional to the surface area [18] while pore size distribution along with other parameters (e.g., characteristics of the adsorbates) also plays important roles in adsorption capacity. [19] Overall, HiPco BP had the highest surface area and the smallest pore diameter of the BPs fabricated, regardless of degassing. Among AD BPs, methanol-cleaned BPs had the highest surface area with minimal difference in the average pore width. A long degassing process improved surface area for acetone-cleaned and methanol-cleaned AD BPs while non-cleaned AD BPs and HiPco BPs showed no improvement. For HiPco SWNTs which did not contain surfactants the degassing process did not show improvement. The cleaning process as well as the extended degassing of the AD SWNTs helped remove some impurities and using methanol resulted in slightly more adsorptive material than using acetone. Cinke et al. reported 567 m^2/g surface area with 7.4 nm average pore diameter of HiPco SWNTs (22 wt % as Fe) and a high increased surface area to 1587 m^2/g with decreased average pore width (3.9 nm) after two step purification process consisting of dimethylformamide/ethylene diamine treatment (first step) and HCl treatment and wet air oxidation at 225 ˚C for 18 hr (second step). [20] Yang et al. obtained 524 m^2/g surface area (3.5 nm average pore diameter) with HiPco SWNTs and observed an increased surface

area of 861 m²/g after air oxidation at 350 ˚C for 30 min followed by HCl washing. [21] With an additional annealing at 600 ˚C after HF treatment, the surface area of HiPco SWNTs was measured as high as 1555 m²/g. [22] Raw AD SWNTs were measured to have 376 m²/g and HCl treatment increased it to 483 m²/g. [23] Few experimental data on surface area of packed/bundled form of CNTs such as BP has been reported in the literature. [24-26] Sweetman et al. fabricated HiPco SWNT BPs through filtration method using macrocyclic ligands (β-cyclodextrin sulphated sodium salt (β-CD), 4-sulfonic calix[6]arene hydrate (C6S), meso-tetra(4-sulfonatophenyl)porphyrin dihydrogen chloride (TSP), and phthalocyanine tetrasulfonic acid (PTS)) for suspension and using water and methanol for washing. [24] Surface area was found to be from 30 to 690 m²/g (2 – 27 nm mean pore diameter), with BP suspended in β-CD having the highest surface area. The same group further fabricated CVD MWNT BPs through the same fabrication process but with dispersants, including C6S, TSP, and PTS. [25] Surface area was in the range of 180 to 250 m²/g (20-26 nm pore diameter). BP fabricated with C6S showed the highest surface area (250 m²/g) which was however much lower than the previously examined SWNT BP fabricated with the same dispersant (580 m²/g). Li et al. performed computational modelling studies on BPs made of (5,5) SWNTs and mean pore size tended to be decreasing from 6.4 to 8.4 nm as the SWNT length increased from 50 to 2000 nm, which is in the same order of magnitude with our studies as well as most available literature. [27, 28]

As described above, differences in the surface area of CNT are often found. CNTs are broadly categorized into SWNTs and multi-walled carbon nanotubes (MWNTs) [29] and also depending on the synthesis method each can be further categorized (e.g., CVD,

AD, laser ablation, HiPco (only producing SWNTs)) [29-31], which makes a difference in their physical and chemical properties. The exact type of CNT is not always available in the literature, different forms of CNTs (e.g. powder, solution, BP, etc.) are used, and various BP fabrication methods are employed. Because of these circumstances there has not been an agreement on the magnitude of the surface area for each type of CNTs. In this study, we sought to determine which SWNT BP, AD or HiPco, has better adsorption properties, but our AD SWNTs were already suspended using surfactant in water which could have also contributed to the difference in this study. SWNTs in general are available in a variety of purity levels, but the same purity level is not always available in different types of SWNT. Most purification processes modify the physical and chemical properties of SWNTs by introducing defects in the tube walls and adding functional groups such as –COOH or –OH to the defects and tube ends. [32] Our approach in this study was to maintain the physical/chemical integrity of the SWNT substrates as much as possible by not challenging them with harsh conditions such as high temperature peroxide or acid digestion. We found that suspending CNTs in surfactants can negatively affect the BET surface area which can be corrected to varying degrees with solvent cleaning or extended degassing.

Toluene Adsorption Capacity

Toluene adsorption isotherms obtained with the DAIC system are shown in Figure 4. Adsorption capacities were determined at 800 ppm equilibrium concentration and found to be 25, 34, 46 and 106 mg toluene/g BP for non-cleaned AD, acetone-cleaned AD,

methanol-cleaned AD and HiPco BPs, respectively. The two samples sent to Micromeritics® for verification of DAIC performance (acetone-cleaned and methanol-cleaned AD BPs) were degassed for a much longer time than was our practice (960 min vs. 60 min) and were found to have much greater toluene adsorption capacity, 616 and 768 mg/g, respectively. When these same samples were re-measured using the DAIC system we found adsorption capacities to be 443 and 518 mg/g at 800 ppm for acetone-cleaned and methanol-cleaned AD BPs, respectively (Figure 4).

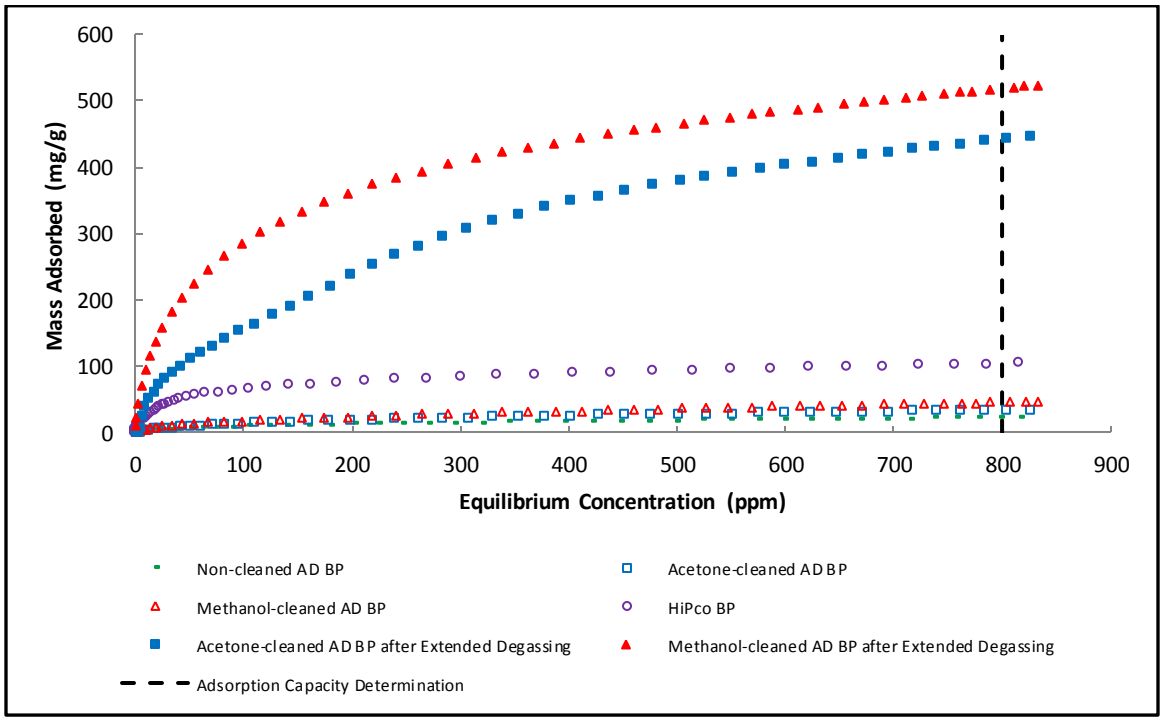

Figure 4. Toluene Adsorption Isotherms Obtained with DAIC System at 30 ˚C

The toluene adsorption capacities obtained through our DAIC system and the physisorption analyzer were overall similar to each other with differences likely due to two major differences in experimental conditions. Adsorption capacities from the

physisorption analyzer were at an equilibrium concentration of 28500 ppm at 25 ˚C while results from our DAIC system were from an equilibrium concentration of 800 ppm and 30 ˚C. At higher concentration and lower temperature adsorption capacity is expected to be larger, as was observed in these results.

Notwithstanding, higher toluene adsorption capacity was observed in materials with higher surface area. Adsorption capacities of the samples treated with extended degassing (300 ˚C for 960 min) showed greatly improved adsorption capacity (12 – 13 fold increase over solvent cleaning alone), but only modest increases in BET surface area.

CNTs have been extensively investigated for their adsorption for hydrogen storage [33-35] and more recently, literature has shown the use of CNTs in organic compound adsorption [14, 36, 37]. Adsorption capacity of AD and HiPco SWNTs were examined with several VOCs and toluene was the greatest followed by methyl ethyl ketone (MEK), hexane, and cyclohexane for both types of SWNTs. [14] HiPco SWNTs exhibited higher adsorption capacity (average 356 mg/g) than AD SWNTs (average 216 mg/g) for all VOCs examined. Other organic compounds which have been tested include carbon tetrachloride (CCl_4) with AD SWNTs [36] and hydrocarbons, including ethanol, iso-propanol, cyclohexane, cyclohexene, benzene, and n-hexane, with SWNTs (not specified) [37]. Due to high flexibility, CNT films (i.e., transparent and conductive films, TCFs) have been extensively investigated for electronic device applications.[16, 38-40] SWNT films were successfully optimized in terms of in surface smoothness and sheet resistance as hole-injection electrodes for organic light-emitting diodes (OLEDs). [39] Superior transmittance spectrum of a SWNT film indicated broad applicability in photonic devices. [16] Gas-, bio- sensor and analytical technology is another promising

field of CNT film/BP application. [38, 41-44] Thin-film transistors constructed from SWNTs were tested with dimethyl methylphosphonate and they were able to detect sub-ppb concentration levels. [41] HiPco SWNT BP was examined as an organic preconcentrator and significant affinity to the tested vapors (toluene, methyl ethyl ketone, and dimethyl methylphosphonate) was observed when thermally desorbed. [43] CVD CNT film deposited in a capillary tube showed high adsorption and fast desorption with high-resolution separation of toluene and hexane. [44] CNT film/BP has also been studied in the water purification and filtration applications. [25, 45, 46] MWNT BP successfully removed trace organic contaminants in solution and dispersants used to fabricate BP played an important role in the removal efficiency. [25] Most adsorption studies of organic compounds as well as inorganics, however, have been performed in solution mainly for water treatment application with CNT powder.[47, 48] Adsorption and desorption characteristics of BP as well as CNT powder using other organic compounds need to be explored further.

Mechanical Properties of BP

Methanol-cleaned AD BP and HiPco BP had tensile strength of 59 and 8 MPa and Young's modulus (E) of 11.4 and 1.3 GPa, respectively.

The superior mechanical properties of the methanol-cleaned AD BP could result from parameters like type of CNTs and fabrication procedure (surfactant/solvent, cleaning, etc.) and as shown in this study literature reports a somewhat wide range of data. [25, 49-52] Zhang et al. used BPs fabricated with 100 mg HiPco SWNTs in nitric acid

dispersion and the highest acid-concentrated (10 M) BP showed the highest tensile strength and E; 74 MPa and 5.0 GPa, respectively. [51] Sweetman et al. also tested HiPco SWNT BPs fabricated using different dispersants (β-CD, C6S, TSP, and PTS). [24] The measured tensile strength was from 6 to 18 MPa, and E was from 0.6 to 2.0 GPa, with PTS the second highest in tensile strength (15 MPa) and the highest in E (2.0 GPa). In a further study, the group examined CVD MWNT BP fabricated with dispersants including C6S, TSP, and PTS. [25] Tensile strength was from 2.5 to 13 MPa and E was from 0.3 to 1.2 GPa, with PTS suspended BP the highest in both properties. Malik et al. performed a tensile test for laser ablation SWNT BPs and obtained 10 to 24 MPa, depending on the purification procedure. [52] Computational studies on E have found to be comparable with experimental results. [27, 53] (5,5) SWNT BPs with different tube lengths (50 – 2000 nm) showed E ranging from 0.1 to 0.3 GPa; the shortest having the highest E. [27] Cranford et al. modelled (5,5) SWNT BP and reported 0.2 – 1.4 GPa, E increasing by decreasing porosity. [53] In fact, BPs used in our study for the mechanical test were fabricated with only half mass of the original BPs used in adsorption experiments and the mechanical properties of those BPs are expected to be higher than the obtained data due to increased thickness. Surfactant or solvent effect on mechanical strength/flexibility also has to be further addressed.

CONCLUSIONS

We fabricated structurally sturdy BPs through vacuum filtration method for PTD application. The solvent cleaning process increased BET surface area and decreased

average pore diameter for AD BPs. We have observed that the extended high temperature degassing increased the surface area and toluene adsorption capacity of AD BPs, suggesting that the cleaning process did not completely remove surfactant residues. Adsorption capacity increased with increasing surface area of BPs but toluene capacities were much more increased considering the relatively modest increase in surface area after extended degassing. AD BPs will need heat treatment to improve their adsorption properties. Overall, HiPco BP had the best adsorption properties (i.e., surface area, average pore width, and toluene adsorption capacity) as well as a simpler fabrication process compared with AD BPs, indicating suitability for VOC passive sampling and analysis by PTD.

ACKNOWLEDGEMENTS

This study was supported by the R21 Grant (#1R21OH010373) from National Institute for Occupational Safety and Health (NIOSH). Its contents are solely responsibility of the authors and do not necessarily represent the official views of NIOSH.

REFERENCES

1 **Pristas, R.:** Passive badges for compliance monitoring internationally. *American Industrial Hygiene Association Journal* 55(9): 841 (1994).

2 **Shih-Wei, T., and S.S. Que Hee:** A new passive sampler for regulated workplace ketones. *AIHAJ* 61(6): 808-814 (2000).

3 **Williams, C.E., P.N. Pintauro, and R.J. Rando:** A transient model of mass transfer and kinetics in a passive vapor sampler. *American Industrial Hygiene Association Journal* 56(11): 1074-1082 (1995).

4 **Berlin, A., R.H. Brown, K. Leichnitz, B. Miller, K.J. Saunders, and B. Striefler:** Diffusive Sampling—An Alternative Approach. *Applied Industrial Hygiene* 3(2): R-2-R-6 (1988).

5 **William F. Martin, J.M.L., Timothy G. Prothero:** *Hazardous Waste Handbook for Health and Safety*: Butterworth Publishers, 1987.

6 **Floyd, E.L., K. Sapag, J. Oh, and C.T. Lungu:** Photothermal desorption of single-walled carbon nanotubes and coconut shell-activated carbons using a continuous light source for application in air sampling. *Annals of Occupational Hygiene* 58(7): 877-888 (2014).

7 **Ajayan, P.M., M. Terrones, A. De la Guardia, V. Huc, N. Grobert, B.Q. Wei et al.:** Nanotubes in a flash - Ignition and reconstruction. *Science* 296(5568): 705 (2002).

8 **Mizuno, K., J. Ishii, H. Kishida, Y. Hayamizu, S. Yasuda, D.N. Futaba et al.:** A black body absorber from vertically aligned single-walled carbon nanotubes. *Proceedings of the National Academy of Sciences of the United States of America* 106(15): 6044-6047 (2009).

9 **Pop, E., D. Mann, Q. Wang, K. Goodson, and H. Dai:** Thermal conductance of an individual single-wall carbon nanotube above room temperature. *Nano Letters* 6(1): 96-100 (2006).

10 **Volkov, A.N., and L.V. Zhigilei:** Heat conduction in carbon nanotube materials: Strong effect of intrinsic thermal conductivity of carbon nanotubes. *Applied Physics Letters* 101(4)(2012).

11 **Bacsa, R.R., C. Laurent, A. Peigney, W.S. Bacsa, T. Vaugien, and A. Rousset:** High specific surface area carbon nanotubes from catalytic chemical vapor deposition process. *Chemical Physics Letters* 323(5-6): 566-571 (2000).

12 **Sone, H., B. Fugetsu, T. Tsukada, and M. Endo:** Affinity-based elimination of aromatic VOCs by highly crystalline multi-walled carbon nanotubes. *Talanta* 74(5): 1265-1270 (2008).

13 **Jahangiri, M., S.J. Shahtaheri, J. Adl, A. Rashidi, H. Kakooei, A.R. Forushani et al.:** The adsorption of benzene, toluene and xylenes (BTX) on the carbon nanostructures: The study of different parameters. *Fresenius Environmental Bulletin* 20(4 A): 1036-1045 (2011).

14 **Agnihotri, S., M.J. Rood, and M. Rostam-Abadi:** Adsorption equilibrium of organic vapors on single-walled carbon nanotubes. *Carbon* 43(11): 2379-2388 (2005).

15 **Shi, Z., X. Chen, X. Wang, T. Zhang, and J. Jin:** Fabrication of superstrong ultrathin free-standing single-walled carbon nanotube films via a wet process. *Advanced Functional Materials* 21(22): 4358-4363 (2011).

16 **Wu, Z., Z. Chen, X. Du, J.M. Logan, J. Sippel, M. Nikolou et al.:** Transparent, conductive carbon nanotube films. *Science* 305(5688): 1273-1276 (2004).

17 **NanoIntegris:** "How to Create CNT Thin Films with NanoIntegris CNTs in Aqueous Solution " [Online] Available at http://www.nanointegris.com/en/downloads

18 **Demiral, H., T. Demiral, B. Karabacakoğlu, and F. Tümsek:** Production of activated carbon from olive bagasse by physical activation. *Chemical Engineering Research and Design* 89(2): 206-213 (2011).

19 **Dobre, T., O.C. Paîrvulescu, G. Iavorschi, M. Stroescu, and A. Stoica:** Volatile organic compounds removal from gas streams by adsorption onto activated carbon. *Industrial and Engineering Chemistry Research* 53(9): 3622-3628 (2014).

20 **Cinke, M., J. Li, B. Chen, A. Cassell, L. Delzeit, J. Han et al.:** Pore structure of raw and purified HiPco single-walled carbon nanotubes. *Chemical Physics Letters* 365(1-2): 69-74 (2002).

21 **Yang, C.M., K. Kaneko, M. Yudasaka, and S. Iijima:** Effect of Purification on Pore Structure of HiPco Single-Walled Carbon Nanotube Aggregates. *Nano Letters* 2(4): 385-388 (2002).

22 **Lafi, L., D. Cossement, and R. Chahine:** Raman spectroscopy and nitrogen vapour adsorption for the study of structural changes during purification of single-wall carbon nanotubes. *Carbon* 43(7): 1347-1357 (2005).

23 **Eswaramoorthy, M., R. Sen, and C.N.R. Rao:** A study of micropores in single-walled carbon nanotubes by the adsorption of gases and vapors. *Chemical Physics Letters* 304(3-4): 207-210 (1999).

24 **Sweetman, L.J., L. Nghiem, I. Chironi, G. Triani, M. In Het Panhuis, and S.F. Ralph:** Synthesis, properties and water permeability of SWNT buckypapers. *Journal of Materials Chemistry* 22(27): 13800-13810 (2012).

25 **Rashid, M.H.O., S.Q.T. Pham, L.J. Sweetman, L.J. Alcock, A. Wise, L.D. Nghiem et al.:** Synthesis, properties, water and solute permeability of MWNT buckypapers. *Journal of Membrane Science* 456: 175-184 (2014).

26 **Muramatsu, H., T. Hayashi, Y.A. Kim, D. Shimamoto, Y.J. Kim, K. Tantrakarn et al.:** Pore structure and oxidation stability of double-walled carbon nanotube-derived bucky paper. *Chemical Physics Letters* 414(4-6): 444-448 (2005).

27 **Li, Y., and M. Kröger:** A theoretical evaluation of the effects of carbon nanotube entanglement and bundling on the structural and mechanical properties of buckypaper. *Carbon* 50(5): 1793-1806 (2012).

28 **Li, Y., and M. Kröger:** Computational study on entanglement length and pore size of carbon nanotube buckypaper. *Applied Physics Letters* 100(2)(2012).

29 **Aqel, A., K.M.M.A. El-Nour, R.A.A. Ammar, and A. Al-Warthan:** Carbon nanotubes, science and technology part (I) structure, synthesis and characterisation. *Arabian Journal of Chemistry* 5(1): 1-23 (2012).

30 **M. M. A. Rafique, J.I.:** Production of Carbon Nanotubes by Different Routes - A Review. *J. of Encapsulation and Adsorption Sciences* (1): 29-34 (2011).

31 **Dai, H.:** Carbon nanotubes: Opportunities and challenges. *Surface Science* 500(1-3): 218-241 (2002).

32 **Itkis, M.E., D.E. Perea, S. Niyogi, S.M. Rickard, M.A. Hamon, H. Hu et al.:** Purity evaluation of as-prepared single-walled carbon nanotube soot by use of solution-phase near-IR spectroscopy. *Nano Letters* 3(3): 309-314 (2003).

33 **Liu, C., Y.Y. Fan, M. Liu, H.T. Cong, H.M. Cheng, and M.S. Dresselhaus:** Hydrogen storage in single-walled carbon nanotubes at room temperature. *Science* 286(5442): 1127-1129 (1999).

34 **Dillon, A.C., K.M. Jones, T.A. Bekkedahl, C.H. Kiang, D.S. Bethune, and M.J. Heben:** Storage of hydrogen in single-walled carbon nanotubes. *Nature* 386(6623): 377-379 (1997).

35 **Ye, Y., C.C. Ahn, C. Witham, B. Fultz, J. Liu, A.G. Rinzler et al.:** Hydrogen adsorption and cohesive energy of single-walled carbon nanotubes. *Applied Physics Letters* 74(16): 2307-2309 (1999).

36 **Babaa, M.R., N. Dupont-Pavlovsky, E. McRae, and K. Masenelli-Varlot:** Physical adsorption of carbon tetrachloride on as-produced and on mechanically opened single walled carbon nanotubes. *Carbon* 42(8-9): 1549-1554 (2004).

37 **Bittner, E.W., M.R. Smith, and B.C. Bockrath:** Characterization of the surfaces of single-walled carbon nanotubes using alcohols and hydrocarbons: A pulse adsorption technique. *Carbon* 41(6): 1231-1239 (2003).

38 **Cao, Q., and J.A. Rogers:** Ultrathin films of single-walled carbon nanotubes for electronics and sensors: A review of fundamental and applied aspects. *Advanced Materials* 21(1): 29-53 (2009).

39 **Zhang, D., K. Ryu, X. Liu, E. Polikarpov, J. Ly, M.E. Tompson et al.:** Transparent, conductive, and flexible carbon nanotube films and their application in organic light-emitting diodes. *Nano Letters* 6(9): 1880-1886 (2006).

40 **Azoz, S., A.L. Exarhos, A. Marquez, L.M. Gilbertson, S. Nejati, J.J. Cha et al.:** Highly conductive single-walled carbon nanotube thin film preparation by direct alignment on substrates from water dispersions. *Langmuir* 31(3): 1155-1163 (2015).

41 **Novak, J.P., E.S. Snow, E.J. Houser, D. Park, J.L. Stepnowski, and R.A. McGill:** Nerve agent detection using networks of single-walled carbon nanotubes. *Applied Physics Letters* 83(19): 4026-4028 (2003).

42 **Brady-Estévez, A.S., S. Kang, and M. Elimelech:** A single-walled-carbon-nanotube filter for removal of viral and bacterial pathogens. *Small* 4(4): 481-484 (2008).

43 **Zheng, F., D.L. Baldwin, L.S. Fifield, N.C. Anheier, C.L. Aardahl, and J.W. Grate:** Single-walled carbon nanotube paper as a sorbent for organic vapor preconcentration. *Analytical Chemistry* 78(7): 2442-2446 (2006).

44 **Saridara, C., R. Brukh, Z. Iqbal, and S. Mitra:** Preconcentration of volatile organics on self-assembled, carbon nanotubes in a microtrap. *Analytical Chemistry* 77(4): 1183-1187 (2005).

45 **Sears, K., L. Dumée, J. Schütz, M. She, C. Huynh, S. Hawkins et al.:** Recent developments in carbon nanotube membranes for water purification and gas separation. *Materials* 3(1): 127-149 (2010).

46 **Yu, M., H.H. Funke, J.L. Falconer, and R.D. Noble:** High density, vertically-aligned carbon nanotube membranes. *Nano Letters* 9(1): 225-229 (2009).

47 **Chen, W., L. Duan, and D. Zhu:** Adsorption of polar and nonpolar organic chemicals to carbon nanotubes. *Environmental Science and Technology* 41(24): 8295-8300 (2007).

48 **Fagan, S.B., A.G. Souza Filho, J.O.G. Lima, J. Mendes Filho, O.P. Ferreira, I.O. Mazali et al.:** 1,2-Dichlorobenzene interacting with carbon nanotubes. *Nano Letters* 4(7): 1285-1288 (2004).

49 **Zaeri, M.M., S. Ziaei-Rad, A. Vahedi, and F. Karimzadeh:** Mechanical modelling of carbon nanomaterials from nanotubes to buckypaper. *Carbon* 48(13): 3916-3930 (2010).

50 **Xu, G., Q. Zhang, W. Zhou, J. Huang, and F. Wei:** The feasibility of producing MWCNT paper and strong MWCNT film from VACNT array. *Applied Physics A: Materials Science and Processing* 92(3): 531-539 (2008).

51 **Zhang, X., T.V. Sreekumar, T. Liu, and S. Kumar:** Properties and structure of nitric acid oxidized single wall carbon nanotube films. *Journal of Physical Chemistry B* 108(42): 16435-16440 (2004).

52 **Malik, S., H. Rösner, F. Hennrich, A. Böttcher, M.M. Kappes, T. Beck et al.:** Failure mechanism of free standing single-walled carbon nanotube thin films under tensile load. *Physical Chemistry Chemical Physics* 6(13): 3540-3544 (2004).

53 **Cranford, S.W., and M.J. Buehler:** In silico assembly and nanomechanical characterization of carbon nanotube buckypaper. *Nanotechnology* 21(26)(2010).

HEAT TREATMENT OF BUCKYPAPER (BP) FOR USE IN VOLATILE ORGANIC COMPOUNDS (VOCs) SAMPLING

by

JONGHWA OH, EVAN L. FLOYD, MAHESI PARIT, VIRGINIA A. DAVIS, CLAUDIU T. LUNGU

Submitted to *Journal of Nanomaterials*

Format adapted for dissertation

ABSTRACT

Three types of buckypapers (BPs), two of them fabricated with arc discharge (AD) single-walled carbon nanotubes (SWNTs) (acetone-cleaned AD BP and methanol-cleaned AD BP) and one with high-pressure carbon monoxide (HiPco) SWNTs (HiPco BP), were heat-treated at different conditions to find the specific conditions for each type that improve the adsorption properties. Based on thermogravimetric analysis (TGA) data, three heat-treatment conditions were designed for AD BPs and another three conditions for HiPco BPs. Also, changes in weight and physical integrity before and after the heat treatment were considered. Heating at 300 ˚C for 90 minutes was selected for acetone-cleaned AD BP, in which the BP kept its physical integrity and yielded a relatively high Brunauer, Emmett, and Teller (BET) surface area (970 ± 18 m^2/g), while methanol-cleaned AD BP was excluded because of its physical change. For HiPco BP a condition of 300 ˚C heating for 30 minutes was chosen as a relatively higher surface area (933 ± 54 m^2/g) and less weight loss (5 %) were observed.

INTRODUCTION

Strategies to fabricate CNT films or buckypaper (BP) have been developed mostly for use in electronic devices. [1] Processes such as vacuum filtration, solution spraying, drop casting, and layer by layer assembly have been widely investigated and successfully used. [1, 2] Certain fabrication methods such as vacuum filtration or solution spraying commonly require suspending CNTs in surfactants for obtaining a homogenous solution and after the deposition on a substrate like a membrane filter or glass, rinsing the deposited cake with purified water to remove the surfactants. [1, 3, 4] Surfactants could insulate CNTs and possibly lower their conductivity. [5, 6] Although it is often thought that the surfactants could be completely removed with water rinsing [3, 7], studies have found remained surfactants in SWNT films [5-7]. Additional purification process of surfactants has been suggested such as heat or acid treatments. [5-7]

In our previous study for the application of the photothermal desorption (PTD) [8], arc discharge (AD) and high-pressure carbon monoxide (HiPco) single-walled carbon nanotubes (SWNTs) were fabricated into BPs through the vacuum filtration method, a relatively simple and inexpensive procedure [1, 6]. We determined that the fabrication process left surfactant residues in AD BPs. Since AD SWNTs were pre-suspended in surfactants (i.e., sodium cholate and sodium dodecyl sulfate) when purchased, a cleaning process with DI water and solvent rinsing was involved; however, increased weight of the BP compared with expected was observed even after the cleaning, which was attributed to the residual surfactants left within the fabricated AD BPs.

The purpose of this study was to find the appropriate heat treatment conditions for each type of BP in order to improve adsorption properties by removing surfactants or solvent related impurities. For AD BPs our main purpose was to remove surfactants imbedded in AD BP rather than removing metal impurities, so heat treatment at a mild temperature was performed. Because of the low probability for SWNTs to be oxidized at mild temperatures [6, 9, 10] and simplified furnace operation, heat treatment was performed in air environment. In addition, HiPco BPs were included in this study mainly to remove any impurities involved in the synthesis and fabrication process. Thermogravimetric analysis (TGA) was performed in advance to determine appropriate heat treatment conditions specific to each type of BPs.

EXPERIMENTAL

Buckypaper (BP) Fabrication

The fabrication procedure was adopted from our previous study. [8] Arc discharge (AD) SWNT solution (1 mg/mL, 94.5 % pure) pre-suspended in surfactants (1 % w/v sodium cholate and sodium dodecyl sulfate in water) and HiPco SWNTs (85 % pure) powder were purchased from Nanointegris Inc. (Quebec, Canada). A typical filtration and suspension procedure to fabricate BPs was employed and two fabrication/rinsing methods for AD BP (i.e., acetone-cleaned and methanol-cleaned) and one method for HiPco BP were used. For the fabrication of AD BPs, 50 mL (50 mg) of the AD SWNT suspension was mixed with 400 mL of solvent (either acetone or methanol) for 15 hours. The suspension was then vacuum-filtered through a polytetrafluoroethylene (PTFE)

membrane filter (47 mm diameter, 5 μm pore, EMD Millipore, Darmstadt, Germany) and a series of two alternating rinses were used after the SWNT cake was deposited on the filter but not dried. The SWNT cake was first rinsed with 250 mL of deionized water (18.2 MΩ-cm) then 50 mL of solvent to make either acetone-cleaned or methanol-cleaned AD BP. The deposited cake was allowed to dry for 30 minutes under vacuum plus another 2 hours without vacuum while on the filter membrane and a BP was obtained by delaminating the dried SWNT cake from the filter. For HiPco BP preparation, 50 mg of powdered HiPco SWNTs were suspended in 400 mL methanol and ultra-sonicated using a 490 W bath sonicator (BRANSON CPX5800H, Danbury, CT) for 150 minutes. The solution was vacuum-filtered through the same type of PTFE membrane filter and allowed to dry in the same way as mentioned (30 minutes under vacuum plus another 2 hours without vacuum). The SWNT cake was then delaminated from the filter to obtain a BP.

Thermogravimetric Analysis (TGA)

TGA (Q500, TA Instruments, New Castle, DE) was performed on the fabricated BPs (n=2). A sample was held at 120 ˚C for 20 min to remove of residual moisture and heated to 800 ˚C with a ramping rate of 10˚C/min in air environment, followed by 45 min hold. Based on the data obtained (see result section), further heat treatment conditions were determined. For AD BPs, three conditions were set in which the surfactants were expected to be completely removed without a considerable weight loss compared with the theoretically expected weight (i.e., 50 mg): 300 ˚C for 90 min, 350 ˚C for 60 min, and

300 ˚C 120 min. For the HiPco BPs the treatment conditions were set where the surface area was expected to be increased with a minimal weight loss: 350 ˚C, 300 ˚C, and 250 ˚C for 30 min.

Heat Treatment

Heat treatment was performed with a muffle furnace (Thermolyne™ F48025-60-80, Thermo Fisher Scientific™, Waltham, MA). The ramping rate was 10 ˚C/min and samples were held for the designated conditions (time and temperature) and then cooled down to room temperature. Changes in weight and the physical appearance and integrity were recorded before and after heat treatment.

Characterization of Adsorption Properties

Surface area and pore size were analyzed with a physisorption analyzer (Micromeritics® ASAP 2020, Norcross, GA) using N_2 at 77 K. Samples were degassed for an hour at a temperature in which each sample was heat-treated prior to the measurement. Analysis was duplicated each BP (n=2) and averaged. Brunauer, Emmett, and Teller (BET) theory was used to determine surface area and subsequently mean pore width.

RESURLTS AND DISCUSSION

Thermogravimetric Analysis (TGA)

10 % weight loss of acetone-cleaned AD, methanol-cleaned AD BPs, and HiPco BPs occurred at an average of 295 ± 9, 305 ± 0, and 377 ± 5 ˚C, while 50 % of weight loss occurred at 451 ± 3, 454 ± 1, and 474 ± 1˚C, respectively (Figure 1). Since the weight of the fabricated AD BPs was higher (approximately 30 %) than the expected (i.e., 50 mg) because of the residual surfactants and only 10 mg of each BP were used for TGA, the data was re-scaled considering the original weight of the BPs (Figure 2). The temperature where the weight of AD BPs became 50 mg was re-calculated considering the new scale and resulted in 381 and 362 ˚C for acetone-cleaned and methanol-cleaned AD BPs, respectively. Both AD BPs showed a similar decomposition pattern as expected which led to the same heat treatment conditions.

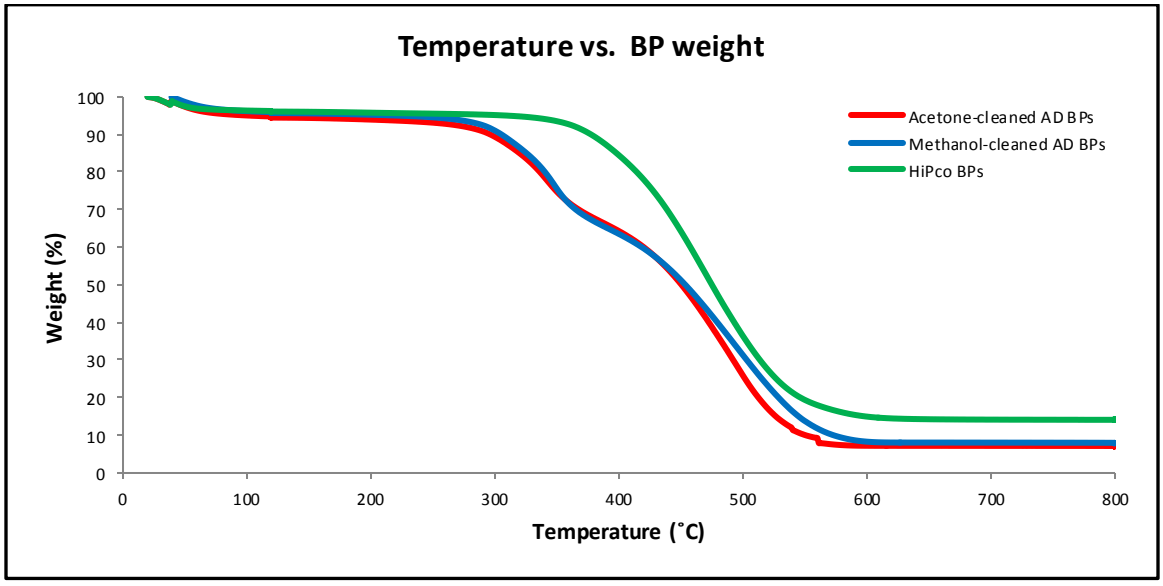

Figure 1. TGA Results for (a) Acetone-cleaned AD BPs, (b) Methanol-cleaned AD BPs, and (c) HiPco BPs

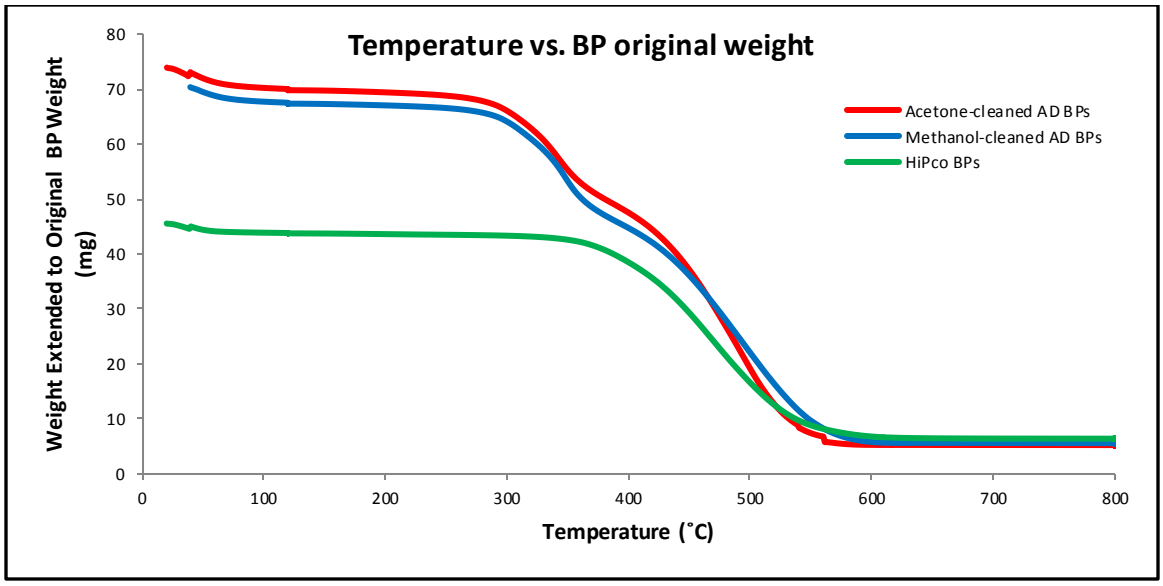

Figure 2. Re-scaled TGA Data

The expected weight of 50 mg is the amount we calculated from the SWNT suspension for AD BPs and the amount we weighted on a scale for the powder form HiPco SWNTs, which may result in variations between BP samples since measuring the exact same amount every time is not possible. We assumed that samples below the theoretical weight will only contain the pure material and surfactants/solvents were all removed. In a study aimed at removing the remnant surfactants and keeping intactness of the CVD SWNT films through differential thermal analyzer and thermogravimetric analysis (DTA-TG), sodium dodecylbenzenesulfonate (SDBS) powder started to decompose at 236 ˚C and a heat treatment at 300 ˚C for 5 hr in air was selected. [6] The temperature (i.e., 300 ˚C) selected was between the oxidation temperature of SWNTs and the starting decomposition temperature of surfactants. Among examined surfactants, removal of SDBS showed the best performance in increasing transparency in CNT films, indicating that heat treatment successfully removed the surfactant. Studies on the removal

of surfactants in transparent and conductive films (TCFs) made of CNTs have been more often reported for applications in electronic devices rather than sampling devices, including the previous study mentioned above. General approaches to remove surfactants to obtain more conductive TCFs include rinsing, heating, acid treatment, etc. AD SWNT film produced by a spray method in which the CNTs were suspended in sodium dodecyl sulfate (SDS), sprayed on polyethylene terephthalate (PET) film, and rinsed in water several times was immersed in various acids and found that HNO_3 could efficiently remove the remaining surfactant. [5] Photocatalysis using ZnO nanoparticles and Fenton reaction were tested to remove surfactants in CVD SWNT film fabricated by filtration method and the removal of residual surfactants was confirmed through Raman and X-ray photoelectron spectroscopy (XPS) spectra. [7] TGA data on pure SDS powder was not found in the literature but it should be expected to decompose at a lower temperature than SDBS which has a higher burning temperature. Few studies have examined TGA with BPs. [11-13] Sweetman et al. performed TGA with HiPco BPs fabricated through *meso*-tetra(4-sulfonatophenyl)porphyrin dihydrogen chloride (TSP) and phthalocyanine tetrasulfonic acid (TPS) suspension in air. [11] The mass of both samples remained relatively constant between 200 and 300 ˚C and showed a sharp decrease between 400 and 600 ˚C which is attributable to the decomposition of the dispersants and SWNTs. This behavior is showing a similar pattern with our study. Muramatsu et al. examined the oxygen stability of CVD double-walled carbon nanotube (DWNT) and SWNT BPs (type not specified) in an argon and oxygen (1 %) mixture. [12] DWNT-derived BP oxidized at a much higher temperature (717 ˚C) compared with SWNT-derived BP. It was observed that the oxidation pattern of the SWNT BP was similar to that of our HiPco BPs.

Heat Treatment

Weight data and images showing the physical appearance of the BPs are shown in Figures 3 and 4, respectively. Acetone-cleaned AD BPs lost approximately 26, 48, and 32 % of their weight, whereas methanol-cleaned AD BPs decreased their weight by around 29, 40, and 34 % at 300 ˚C for 90 min, 350 ˚C for 60 min, and 300 ˚C for 120 min, respectively. HiPco BPs lost about 22, 5, and 1 % at 350 ˚C for 30 min, 300 ˚C for 30 min, and 250 ˚C for 30 min, respectively. However, when we recalculated the weight change from the expected weight of AD BPs considering the surfactant effect, + 5, - 25,

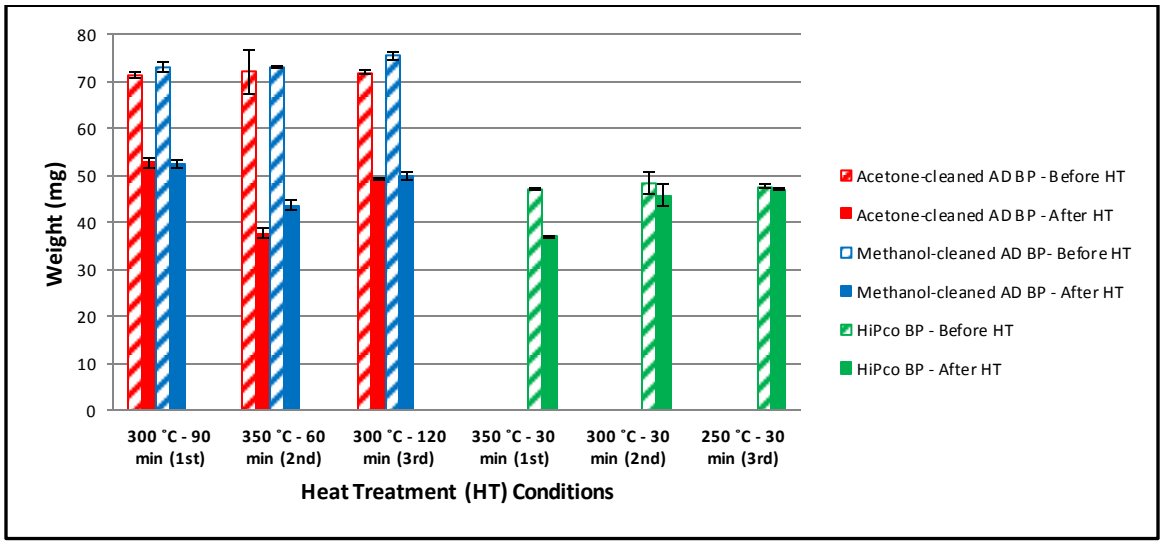

Figure 3. Weight Change Before and After Heat Treatment (HT)

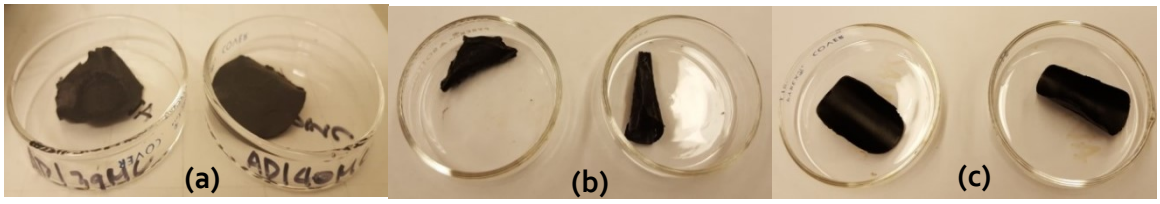

Figure 4. (a) Methanol-cleaned AD BPs before HT, and (b) and (c) Acetone-cleaned AD BPs after HT at 350 ˚C - 60 m and 300 ˚C - 120 m, respectively

and - 2 % weight of acetone-cleaned AD BP were changed after HT at the first (300 ˚C - 90 min), second (350 ˚C - 60 min), and third (300 ˚C - 120 min) conditions while there were + 5, - 13, and 0 % changes in weight for methanol-cleaned AD BPs. As a result, at the first and third conditions, the weight change of AD BPs was minimal while for HiPco BPs weight change was minimal at the second and the third conditions.

Methanol-cleaned AD BPs were either swirled or become brittle even before heat treatment (Figure 4). Acetone-cleaned AD BPs also showed a similar pattern but only at the first condition, they kept the physical integrity. HiPco BPs did not manifest any change in appearance or integrity throughout the experiment and they were very flexible.

Characterization of Adsorption Properties

Acetone-cleaned AD BP had suface area with mean pore width of 970 ± 18 (5.9 ± 0.0), 1228 ± 13 (7.1 ± 0.2), and 1266 ± 7 (5.8 ± 0.2) m^2/g while methanol cleaned AD BP exhibited 1074 ± 10 (5.7 ± 0.0), 1181 ± 31 (6.6 ± 0.2), and 1227 ± 33 (6.0 ± 0.1) m^2/g at the first, second, and third heat treatment conditions, respectively (i.e., 300 ˚C - 90 min, 350 ˚C - 60 min, and 300 ˚C - 120 min). HiPco BP resulted in 887 ± 32 (6.6. ± 0.1), 993 ± 54 (5.6 ± 0.2), and 697 ± 3 (6.2 ± 0.1) m^2/g at the first, second, and third conditions, respectively (i.e., 350 ˚C - 30 min, 300 ˚C - 30 min, and 250 ˚C - 30 min). Figure 5 compares the BET surface area between BPs at different heat treatment conditions. Overall, acetone-cleaned and methanol-cleaned AD BPs revealed a similar pattern at all

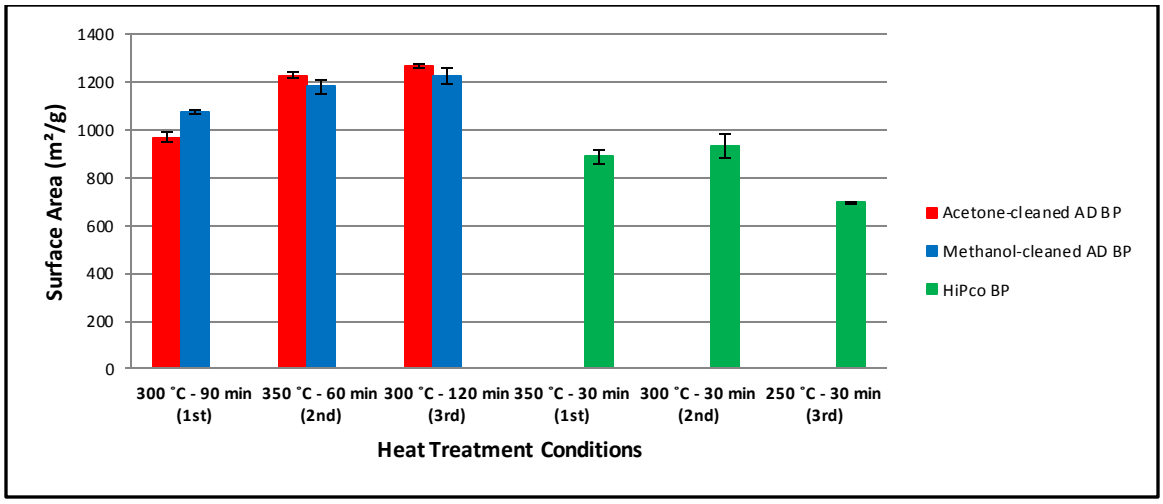

Figure 5. Surface Area Comparison

conditions as expected and all conditions yielded a high BET surface area of almost 1000 m²/g or more which is much higher (at least 2.5 times) than before the heat treatment, 322 and 387 m²/g for acetone-cleaned and methanol-cleaned AD BPs, respectively. At the second (350 ˚C - 60 min) and third (300 ˚C - 120 min) conditions, both AD BPs showed a relatively higher surface area than at the first condition (300 ˚C - 90 min). For HiPco BPs, the first (350 ˚C - 30 min) and second (300 ˚C - 30 min) conditions resulted in a relatively higher surface area while the surface area at the third condition (250 ˚C - 30 min) was not much changed compared to before treatment, 649 m²/g.

Since methanol-cleaned AD BPs did not keep their structural integrity during the experiment, only acetone-cleaned AD BPs were considered to be chosen for our next study in which BPs treated with the selected heat treatment conditions will be examined for desorption efficiency through photothermal desorption (PTD). Although the surface area of the acetone-cleaned AD BPs was relatively lower at the first condition (300 ˚C - 90 min), the condition was selected since the samples were physically intact only at that

condition and weight change was minimal. On the other hand, the second condition (300 ˚C - 30 min) was selected for HiPco BPs because of the minimal loss in weight and relatively high surface area.

Many studies on the purification of CNT powder through chemical, physical, or a combination of both processes are focused on the removal of metal catalysts and carbonaceous impurities in CNTs [14] and as far as we know this study is the first investigation of the heat treatment effect on BPs to improve the adsorption properties by mainly removing surfactant residues and any impurities involved in the process. From our previous study it was suggested that surfactants were not completely removed even after cleaning during the fabrication process mainly due to the long period of suspension while they were stored. Most purification studies employ a combined process of acid treatment (i.e., liquid-phase oxidation) followed by gas-phase oxidation under heat. [14-18] HiPco SWNTs (528 m^2/g) were purified with acids and heat treatment was selectively performed. [15] Among four acids examined (HCl, HF, H_2SO_4, and HNO_3) HF treated SWNTs for 4 – 8 hours yielded 635 m^2/g while HF treatment followed by 600 ˚C heat treatment for 6 hours in inert atmosphere showed the highest increase in surface area (1555 m^2/g). However further heat treatment at 1000 ˚C for 6 hours diminished it to 806 m^2/g, eliminating porous structure. In another study, after the heat treatment of SWNTs (not specified, 298 m^2/g) at 800 ˚C for 2 hours in CO_2 and H_2 environments, surface area was increased to 249 and 351 m^2/g, respectively. 52 and 30 % of weight loss occurred in CO_2 and H_2 environments, respectively, while keeping the original pore size distribution of the SWNTs. [16] On the other hand, nitric acid treatment at 70˚C for 5 hours changed it completely, resulting in surface area of 544 m^2/g.

Heat treatment in air could have oxidized our samples which possibly changed the chemical property or functionalized the materials but we believe that oxidation was minimal in our study since it was performed in a small sized furnace with only a small vent in which air circulates naturally and in a temperature below which the oxidation of SWNTs powder starts (380 – 400 ˚C) [6, 9, 10]. A detailed chemical analysis was not performed in this study to determine if all impurities are completely eliminated through the heat treatment; rather, we used a gravimetric method, which did not give us accurate information on the effect of heat treatment in terms of chemical composition. Since the scope of this study was to find a simple way to remove impurities involved in the fabrication process of BP in order to improve adsorption property, surface area analysis was the focus rather than elemental analysis.

CONCLUSIONS

The effect of heat treatment on the adsorption property was examined on the fabricated AD BP and HiPco BP. Considering the data on surface area and changes in weight and physical integrity before and after heat treatment, conditions at 300 ˚C for 90 min and 300 ˚C for 30 min were determined to be the most appropriate for acetone-cleaned AD BP and HiPco BP, respectively. With those selected conditions, further investigations on photothermal desorption will be followed.

ACKNOWLEDGEMENTS

The research presented in this manuscript was partially supported by NIOSH through an R21 grant (1 R21 OH010373). Any opinions, findings, and conclusions or recommendations expressed in this material are those of the authors and do not necessarily reflect the views of National Institute for Occupational Safety and Health (NIOSH) or represent an endorsement by NIOSH.

REFERENCES

1 **Shi, Z., X. Chen, X. Wang, T. Zhang, and J. Jin:** Fabrication of superstrong ultrathin free-standing single-walled carbon nanotube films via a wet process. *Advanced Functional Materials* 21(22): 4358-4363 (2011).

2 **Di, J., D. Hu, H. Chen, Z. Yong, M. Chen, Z. Feng et al.:** Ultrastrong, foldable, and highly conductive carbon nanotube film. *ACS Nano* 6(6): 5457-5464 (2012).

3 **Wu, Z., Z. Chen, X. Du, J.M. Logan, J. Sippel, M. Nikolou et al.:** Transparent, conductive carbon nanotube films. *Science* 305(5688): 1273-1276 (2004).

4 **Kaempgen, M., G.S. Duesberg, and S. Roth:** Transparent carbon nanotube coatings. *Applied Surface Science* 252(2): 425-429 (2005).

5 **Geng, H.Z., K.K. Ki, P.S. Kang, S.L. Young, Y. Chang, and H.L. Young:** Effect of acid treatment on carbon nanotube-based flexible transparent conducting films. *Journal of the American Chemical Society* 129(25): 7758-7759 (2007).

6 **Wang, J., J. Sun, L. Gao, Y. Liu, Y. Wang, J. Zhang et al.:** Improving the conductivity of single-walled carbon nanotubes films by heat treatment. *Journal of Alloys and Compounds* 485(1-2): 456-461 (2009).

7 **Wang, J., J. Sun, L. Gao, Y. Wang, J. Zhang, H. Kajiura et al.:** Removal of the residual surfactants in transparent and conductive single-walled carbon nanotube films. *Journal of Physical Chemistry C* 113(41): 17685-17690 (2009).

8 **Oh, J., E.L. Floyd, T.C. Watson, and C.T. Lungu:** Fabrication and adsorption characterization of single-walled carbon nanotube (SWNT) buckypaper (BP) for use in air samplers. *Analytical Methods* 8(21): 4197-4203 (2016).

9 **Liu, Y., L. Gao, J. Sun, S. Zheng, L. Jiang, Y. Wang et al.:** A multi-step strategy for cutting and purification of single-walled carbon nanotubes. *Carbon* 45(10): 1972-1978 (2007).

10 **Gajewski, S., H.E. Maneck, U. Knoll, D. Neubert, I. Dörfel, R. Mach et al.:** Purification of single walled carbon nanotubes by thermal gas phase oxidation. *Diamond and Related Materials* 12(3-7): 816-820 (2003).

11 **Sweetman, L.J., L. Nghiem, I. Chironi, G. Triani, M. In Het Panhuis, and S.F. Ralph:** Synthesis, properties and water permeability of SWNT buckypapers. *Journal of Materials Chemistry* 22(27): 13800-13810 (2012).

12 **Muramatsu, H., T. Hayashi, Y.A. Kim, D. Shimamoto, Y.J. Kim, K. Tantrakarn et al.:** Pore structure and oxidation stability of double-walled carbon nanotube-derived bucky paper. *Chemical Physics Letters* 414(4-6): 444-448 (2005).

13 **Sreekumar, T.V., T. Liu, S. Kumar, L.M. Ericson, R.H. Hauge, and R.E. Smalley:** Single-wall carbon nanotube films. *Chemistry of Materials* 15(1): 175-178 (2003).

14 **Hou, P.X., C. Liu, and H.M. Cheng:** Purification of carbon nanotubes. *Carbon* 46(15): 2003-2025 (2008).

15 **Lafi, L., D. Cossement, and R. Chahine:** Raman spectroscopy and nitrogen vapour adsorption for the study of structural changes during purification of single-wall carbon nanotubes. *Carbon* 43(7): 1347-1357 (2005).

16 **Hu, Y.H., and E. Ruckenstein:** Pore Size Distribution of Single-Walled Carbon Nanotubes. *Industrial and Engineering Chemistry Research* 43(3): 708-711 (2004).

17 **Yang, C.M., K. Kaneko, M. Yudasaka, and S. Iijima:** Effect of Purification on Pore Structure of HiPco Single-Walled Carbon Nanotube Aggregates. *Nano Letters* 2(4): 385-388 (2002).

18 **Chiang, I.W., B.E. Brinson, A.Y. Huang, P.A. Willis, M.J. Bronikowski, J.L. Margrave et al.:** Purification and characterization of single-wall carbon nanotubes (SWNTs) obtained from the gas-phase decomposition of CO (HiPco process). *Journal of Physical Chemistry B* 105(35): 8297-8301 (2001).

PHOTOTHERMAL DESORPTION (PTD) OF BUCKYPAPER (BP) FOR USE IN AIR SAMPLERS

by

JONGHWA OH, EVAN L. FLOYD, CLAUDIU T. LUNGU

In preparation for *Anal. Methods.*

Format adapted for dissertation

ABSTRACT

Two types of buckypaper (BP), arc discharge (AD) and high-pressure carbon monoxide (HiPco), were examined for photothermal desorption (PTD), as an alternative to the current chemical or thermal extraction technique for VOC analysis. BPs were preloaded with 864 μg toluene vapor and desorbed with a pulse of light from a photographic grade xenon lamp. A N_2 flow of 15 mL/min carried the desorbed analyte to a photoionization detector (PID) for quantification. AD BP showed the higher recovery rate ranging from 0.016 ± 0.005 to 0.431 ± 0.159 % at all energy levels examined (1.84 – 7.37 J) and difference in the recovery rate between AD and HiPco BPs was statistically significant at all levels. Desorption was determined to be proportional with the energy of the light pulse allowing for repeated analysis or detail analysis. AD BP has potential to be used as an efficient VOC sorbent in combination with PTD.

INTRODUCTION

Chemical or thermal desorption along with gas chromatography (GC) is a commonly used analytical method for the assessment of VOC exposure. [1, 2] Chemical desorption requires at least 30 minutes of extraction in a toxic solvent (e.g., CS_2) and only a tiny portion (e.g., 0.1%) of the diluted desorbed analyte is analyzed with GC. [3-6] Thus its preferred use is in high exposure situation such as occupational setting. On the other hand, thermal desorption is typically employed when not enough mass is collected onto sorbents (traditionally one shot analysis) and an increased sensitivity is necessary such as environmental samples. Although there has been improvement on analysis repeatability and system integrity, the initial cost of equipment is expensive [1] and system reliability check such as leak tests is recommended whenever used [7]. A pump driven sampling (i.e., active sampling) generally collects enough mass for analysis and thus there is no issue on using either chemical or thermal desorption. Passive sampling (no pump involved) however, relies only on diffusion for sample collection (i.e., less mass), which could result in below limit of detection (LOD) measurement when combined with chemical desorption.

New sample extraction techniques have been explored to overcome these issues. [1, 8-10] Accelerated solvent extraction (ASE) system in which the sample is automatically extracted at high pressure and temperature above boiling point of solvents to improve solvent extraction efficiency has been examined for various environmental samples

including VOCs. [1, 8] Alternative solvent use, short extraction time, and simple sample preparation are advantages but high cost of equipment and extracts clean-up are disadvantages. [1, 9] Solid phase microextraction (SPME) enables a single step for sampling and pre-concentration (no focusing trap) followed by direct transfer of analytes into GC.[10, 11] In the SPME system, silica fiber coated with extracting polymer is housed in a needle which is injected into GC for analysis where the fiber is exposed to carrier gas. Fast, sensitive, and inexpensive system are the advantages, while slow partition equilibrium for low volatile compounds and poor storage stability are disadvantages. [2]

Our group recently developed a new desorption technique called photothermal desorption (PTD) in which a pulse of light thermally desorbs the analyte captured on a sorbent. The desorbed analyte could be quantified or qualified by an analytical equipment such as a photoionization detection (PID) or portable GC in the field. [12] PTD eliminates time consuming and expensive laboratory analysis and the use of toxic chemicals. The low sensitivity of chemical desorption for passive samplers collecting low mass can be improved with PTD, and sorbents are reusable. Since only a portion of the analyte is desorbed at once, repeated analysis or further detail analysis is possible.

In our studies [12-14], single-walled carbon nanotubes (SWNTs) have been examined as sorbents for PTD because of large surface area [15, 16], excellent thermal conductivity [17-19], strong mechanical properties as well as great light absorption [20]. PTD was initially examined only with chemical vapor deposition (CVD) SWNTs in powder and felt (loosely bound SWNTs on a filter) form, which was not the most appropriate to be used as a substrate in passive air samplers. [12, 13] In a following study, a sturdy, self-supporting form of carbon nanotubes (CNTs) called buckypaper (BP) was fabricated and

tested for adsorption properties. [14] Two types of SWNTs including arc discharge (AD) and high-pressure carbon monoxide (HiPco) were used, and the fabricated BPs were further heat-treated to improve their adsorption properties.

This study was aimed to examine PTD of the heat-treated BPs using toluene as a representative VOC. A pulse of light was used to desorb toluene from two type of preloaded BPs at different energy levels.

EXPERIMENTAL

Fabrication of Buckypaper (BP)

The BP fabrication procedure was adopted from our previous studies using vacuum filtration method. [14] Arc discharge (AD) SWNT solution (1 mg/mL, 94.5 % pure) which was suspended in surfactants (1 % w/v sodium cholate and sodium dodecyl sulfate in water) and HiPco SWNTs powder (85 % pure) were purchased from Nanointegris Inc. (Quebec, Canada). For the fabrication of AD BPs, 50 mL (50 mg) of the AD SWNT suspension was mixed with 400 mL of acetone for 15 hours. The suspension was then vacuum-filtered through a polytetrafluoroethylene (PTFE) membrane filter (47 mm diameter, 5 μm pore, EMD Millipore, Darmstadt, Germany) and a series of two alternating rinses were administered after the SWNT cake was deposited on the filter but still wet. The SWNT cake was first rinsed with 250 mL of deionized water (18.2 MΩ-cm) then 50 mL of acetone. The deposited cake was allowed to dry for 30 minutes under vacuum plus another 2 hours without vacuum while on the filter membrane and a BP was obtained by delaminating the dried SWNT cake from the filter.

For HiPco BP preparation, 50 mg of powdered HiPco SWNTs were suspended in 400 mL methanol and ultra-sonicated using a 490 W bath sonicator (BRANSON CPX5800H, Danbury, CT) for 120 minutes. The solution was vacuum-filtered through the same type PTFE membrane filter and allowed to dry in the same way as mentioned (30 minutes under vacuum plus 2 hours without vacuum). The SWNT cake was then delaminated from the filter to obtain a BP. The fabricated AD BPs were heat-treated at 300 ˚C for 90 minutes and the HiPco BPs were heated at 300 ˚C for 30 min in a muffle furnace (Thermo Fisher Scientific™, Thermolyne™ F48025-60-80, Waltham, MA) to improve adsorption properties. Those conditions were selected from our previous study to find the best condition for each type of BPs at which both surface area and physical integrity were kept in a reasonable range resulting in improved adsorption properties.

Light Energy

A photographic grade xenon flash lamp (NEEWER® C-250, Neewer Technology ltd., Guangdong, China) was used as a light source and its energy density was measured with a light meter and a thermal sensor (OPHIR Photonics Nova II meter and L50(150)A-LP1-35 sensor, North Logan, UT). Four energy levels were chosen such that the lowest energy density was doubled, tripled, and quadrupled to the next levels. Target energy densities were set at 0.181, 0.362, 0.543 and 0.724 J/cm² based on the maximum deliverable energy. The corresponding energy densities were set by changing power settings on the flash lamp. Energy density was measured prior to each experiment.

Since the light energy is converted to heat energy, material and analyte degradation could be a concern. A temperature at which our material/analyte approaches the highest energy applied, 0.724 J/cm² (i.e., 7.37 J considering the size of BP, 3.6 cm in diameter), was calculated. First, extrapolation of specific heat (Cv) was performed based on Hone's et al.'s experimental data [21]. The specific heat of approximately 650 J/kg·˚C at 26.85 ˚C reported using 9.5 mg laser ablation SWNTs was used and extended to a higher temperature range with a linear regression equation (y = 2.1665x + 639.55, blue straight line in Fig. 1). Based on the data, heat energy (Q) was calculated with Equation (1) (the red parabolic line in Fig. 1). Therefore, when 0.724 J/cm² of energy is applied to a 3.6 cm diameter BP, the temperature of the material/analyte would increase by 177 ˚C above the room (experimental) temperature.

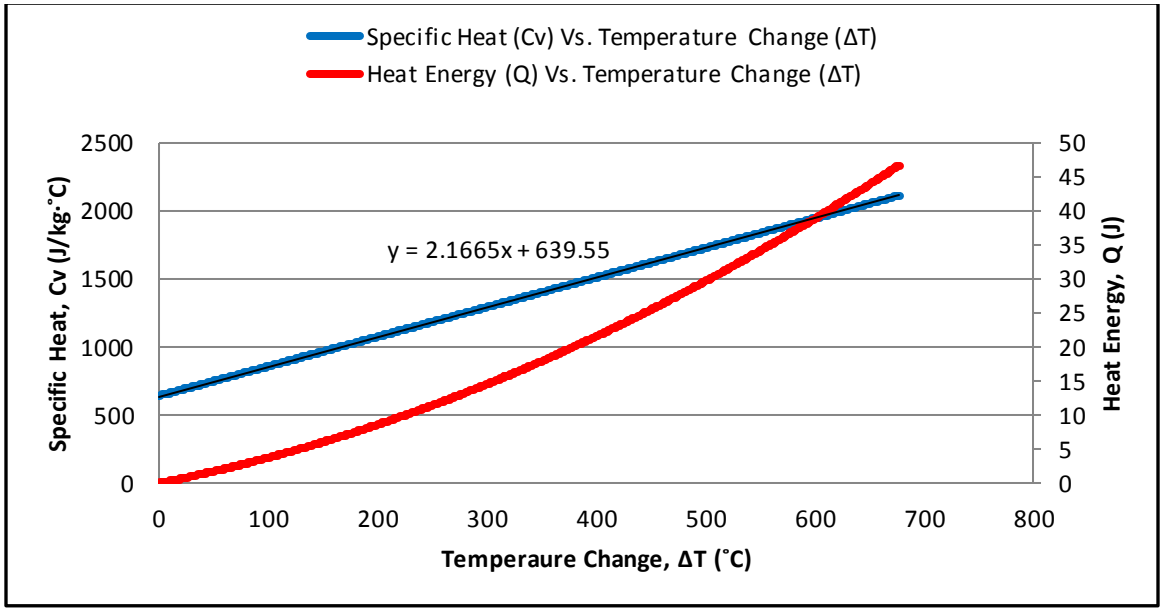

Figure1. Estimation of Incident Heat Energy

$$Q = C_v \times m \times \Delta T \quad (1)$$

where Q is heat energy (J); Cv is specific heat (J/kg·˚C); m is mass (kg); ΔT is change in temperature (˚C).

Sample Loading

Indirect vapor dosing was selected for sample loading, which better represents samples collected for personal exposure assessment, allowing homogeneous adsorption of adsorbates onto sorbents. [12, 22] 864 μg of toluene (Fisher Scientific Certified ACS, Pittsburgh, PA) was injected on the side walls of a glass chamber (130 mL) with a microliter syringe, allowing fast evaporation of the toluene and creating a constant concentration of toluene around the sorbent. The BP sorbent was placed in the chamber with the lid on at room temperature for five hours prior to analysis to allow full adsorption of toluene.

Desorption

A lab designed desorption unit was used for the PTD experiment as shown in Figure 2. A BP sample was place in an approximately 5.75 cm³ aluminum chamber that sits below the xenon flash lamp. Light pulses delivered by the lamp penetrated through the top glass window (0.3 cm thick) and irradiated the BP sorbent sitting in the chamber. The heat generated by the light absorption desorbed the toluene from the BP which was carried by N_2 gas (Ultra High Purity, Airgas, Radnor, PA) flow at 15 mL/min to a PID. A

mass flow controller (SCOTT™ 36A, Plumsteadville, PA) was used to maintain a constant N_2 flow at an exchange rate of 2.6/min. The quantification of desorbed analyte was performed by integrating the peak area from PID data signal, converting it to mass desorbed. The percentage of the desorbed toluene was obtained by dividing the desorbed mass by the toluene mass administered (864 µg). Four replicate measurements were performed at each energy level and results averaged.

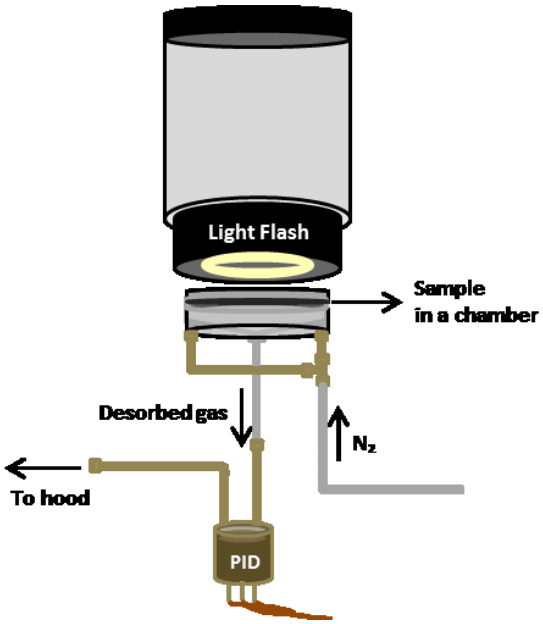

Figure 2. Desorption Unit

Statistics

JMP®12 (SAS, Cary, NC) was used to compare the desorption between two types of BPs (AD and HiPco). Statistical t-test was used and $p < 0.05$ was set to determine statistically significant differences.

RESULTS AND DISCUSSION

Table 1 shows desorption calculated at each energy level for those two types of BPs. As expected as light energy increased the desorption increased as well. Overall, AD BPs showed higher desorption at all energy levels examined compared with HiPco BPs. Desorption for AD BPs ranged from 0.016 ± 0.005 % to 0.431 ± 0.159 % while for HiPco BPs desorption was from 0.001 ± 0.000 % to 0.102 ± 0.006 %. Difference in percent desorption between AD and HiPco BPs was statistically significant at all energy levels; p-values < .0081, .0106, .0007, and .0256 at 1.84, 3.68, 5.53, and 7.37 J, respectively. At the lowest energy level, the coefficient of variation (C.V.) for AD BPs was almost 2 times lower than for HiPco BPs (31 % vs. 63%) whereas at the highest energy level, the C. V. for HiPco BPs was 6 times lower than for AD BPs (6 % vs. 37 %).

Table 1. Comparison of Desorption

		Light Energy (J)			
		1.84	3.68	5.53	7.37
AD BP	Desorption (%)	0.016 ± 0.005	0.102 ± 0.031	0.223 ± 0.031	0.431 ± 0.159
	Desorption (μg)	0.139 ± 0.043	0.883 ± 0.266	1.924 ± 0.269	3.721 ± 1.375
HiPco BP	Desorption (%)	0.001 ± 0.000[1]	0.016 ± 0.004	0.058 ± 0.012	0.102 ± 0.006
	Desorption (μg)	0.004 ± 0.003	0.138 ± 0.033	0.498 ± 0.105	0.879 ± 0.056

[1] 0.0005 ± 0.0003 when not rounded

The relatively high standard deviation and C. V. for desorption were closely related to the energy variation. From our measurements we knew that energy density delivered to the chamber was not exactly the same all the time. The change of energy density was manually controlled by turning the knob on the flash unit. We tried to find

the same spot of the knob to keep identical energy but this was not possible all the time. Also, the lamp had to be re-positioned atop of the desorption chamber every time a BP sample was replaced. The small difference in the position could induce change in the distance between the lamp and the chamber, consequently slightly changing the energy delivered to samples.

In our previous study, three types of samples including CVD SWNTs powder (SWNT-p, + 90 % pure), felt (SWNT-f, loosed deposited on a filter), and activated charcoal powder (AC-p) were examined for PTD. 435 μg toluene vapor were preloaded on 20 mg of each sorbent which was then irradiated with ten flashes at four energy levels (0.78, 1.88, 3.01, and 4.77 J), using a photographic grade xenon flash lamp. [13] At all energy levels, SWNT-f had significantly higher desorption; 0.25 to 3.76 μg (0.057 – 0.864 %) after the first flash and 1.79 to 33.53 μg (0.411 – 7.708 %) after the ten flashes. Li et al. tested 0.65 g CVD multi-walled carbon nanotubes (MWNTs) packed in a stainless steel tube for VOC adsorption and thermal desorption. [23] A 16 VOCs mixture consisted of benzene, toluene, p-xylene, o-xylene, ethylbenzene, n-pentane, n-hexane, cyclohexane, n-heptane, dichloromethane, trichloromethane, acetone, ether, ethyl acetate, n-propanol, and n-butanol was created. A VOC trap was heated to 250 ˚C and the desorbed VOCs were carried by N_2 to GC equipped with flame ionization detector (FID). Recovery rate for all VOCs examined was determined to be 82 to 110 %. Compounds having a relatively lower boiling point seemed to be relatively higher in recovery, with toluene having 103 % recovery rate. Saridara et al. fabricated a microtrap (self-assembled CVD CNTs film on the inside walls of a steel capillary) for adsorption and thermal desorption of trace organics. [24] Trapped toluene and hexane vapors were desorbed with

electrical pulses to 300 – 400 ˚C and transferred to FID equipped in GC through N_2. Desorption was completely reversible and the adsorption of toluene was found to be much stronger than hexane. Zheng et al. investigated adsorption and thermal desorption of a HiPco BP with methyl ethyl ketone (MEK), toluene, and dimethyl methylphosphonate (DMMP). [25] A programmed thermal desorption system heated a preconcentrator tube packed with BPs up to 460 ˚C and the tested vapors were detected with a poly(dimethylsiloxane)-coated 8-MHz flexural plate wave (FPW) microsensor at 210, 360, and 420 ˚C for MEK, toluene, and DMMP, respectively. While MEK and toluene were completely desorbed, DMMP was not fully recovered at higher vapor concentrations they examined.

This study was aimed to collect preliminary data for determining parameters and set-up of the desorption unit and has shown limitations of the current design such as limited control of the light energy and distance from the lamp to the chamber. Further examinations with more precise, elaborated set-up should be followed as well as with other VOCs including polar compounds, for which the CNTs would need to be functionalized to meet the polarity requirements. Once enough data will be collected, the desorbed analyte proportional with the collected VOC will be determined so that the method would estimate the air concentration where the sample was collected.

CONCLUSIONS

We examined PTD of heat-treated AD and HiPco BPs with toluene. Desorption was proportional to the energy level and AD BPs showed significantly higher desorption

than HiPco BPs with a single light flash at all energy levels examined. This study implicated that AD BPs can be an effective sorbent to be used for VOC sampling and analysis with PTD.

ACKNOWLEDGEMENTS

This study was supported by the R21 Grant (#1R21OH010373) from National Institute for Occupational Safety and Health (NIOSH). Its contents are solely responsibility of the authors and do not necessarily represent the official views of NIOSH.

REFERENCES

1 **Fabrizi, G., M. Fioretti, and L. Mainero Rocca:** Occupational exposure to complex mixtures of volatile organic compounds in ambient air: Desorption from activated charcoal using accelerated solvent extraction can replace carbon disulfide? *Analytical and Bioanalytical Chemistry* 405(2-3): 961-976 (2013).

2 **Harper, M.:** Sorbent trapping of volatile organic compounds from air. *Journal of Chromatography A* 885(1-2): 129-151 (2000).

3 **NIOSH:** "Manual of Analytical Methods (NMAM), AROMATIC HYDROCARBONS: METHOD 1501." 2003.

4 **NIOSH:** "Manual of Analytical Methods (NMAM), METHYLENE CHLORIDE: METHOD 1005." 1998.

5 **NIOSH:** "Manual of Analytical Methods (NMAM), HALOGENATED HYDROCARBONS: METHOD 1003." 2003.

6 **NIOSH:** "Manual of Analytical Methods (NMAM), ETHYL ACETATE: METHOD 1457." 1994.

7 **Center for Environmental Research Information, O.R.a.D., U.S. EPA:** "Compendium Method TO-17: Determination of Volatile Oragnic Compounds in Ambient Air Using Active Sampling Onto Sorbent Tubes." U.S. EPA: U.S. EPA.

8 **Richter, B.E., B.A. Jones, J.L. Ezzell, N.L. Porter, N. Avdalovic, and C. Pohl:** Accelerated solvent extraction: A technique for sample preparation. *Analytical Chemistry* 68(6): 1033-1039 (1996).

9 **Giergielewicz-Mozajska, H., L. Dabrowski, and J. Namieśnik:** Accelerated solvent extraction (ASE) in the analysis of environmental solid samples - Some aspects of theory and practice. *Critical Reviews in Analytical Chemistry* 31(3): 149-165 (2001).

10 **Koziel, J.A., and J. Pawliszyn:** Air Sampling and Analysis of Volatile Organic Compounds with Solid Phase Microextraction. *Journal of the Air & Waste Management Association* 51(2): 173-184 (2001).

11 **Elke, K., E. Jermann, J. Begerow, and L. Dunemann:** Determination of benzene, toluene, ethylbenzene and xylenes in indoor air at environmental levels using diffusive samplers in combination with headspace solid-phase microextraction and high-resolution gas chromatography-flame ionization detection. *Journal of Chromatography A* 826(2): 191-200 (1998).

12 **Floyd, E.L., K. Sapag, J. Oh, and C.T. Lungu:** Photothermal desorption of single-walled carbon nanotubes and coconut shell-activated carbons using a continuous light source for application in air sampling. *Annals of Occupational Hygiene* 58(7): 877-888 (2014).

13 **Floyd, E.L.:** Photothermal desorption of toluene from single walled carbon nanotube and activated carbon sorbents, pp. 152. Ann Arbor: The University of Alabama at Birmingham, 2013.

14 **Oh, J., E.L. Floyd, T.C. Watson, and C.T. Lungu:** Fabrication and adsorption characterization of single-walled carbon nanotube (SWNT) buckypaper (BP) for use in air samplers. *Analytical Methods* 8(21): 4197-4203 (2016).

15 **Dervishi, E., Z. Li, Y. Xu, V. Saini, A.R. Biris, D. Lupu et al.:** Carbon nanotubes: Synthesis, properties, and applications. *Particulate Science and Technology* 27(2): 107-125 (2009).

16 **Cinke, M., J. Li, B. Chen, A. Cassell, L. Delzeit, J. Han et al.:** Pore structure of raw and purified HiPco single-walled carbon nanotubes. *Chemical Physics Letters* 365(1-2): 69-74 (2002).

17 **Volkov, A.N., and L.V. Zhigilei:** Heat conduction in carbon nanotube materials: Strong effect of intrinsic thermal conductivity of carbon nanotubes. *Applied Physics Letters* 101(4)(2012).

18 **Pop, E., D. Mann, Q. Wang, K. Goodson, and H. Dai:** Thermal conductance of an individual single-wall carbon nanotube above room temperature. *Nano Letters* 6(1): 96-100 (2006).

19 **Yu, C., L. Shi, Z. Yao, D. Li, and A. Majumdar:** Thermal conductance and thermopower of an individual single-wall carbon nanotube. *Nano Letters* 5(9): 1842-1846 (2005).

20 **Mizuno, K., J. Ishii, H. Kishida, Y. Hayamizu, S. Yasuda, D.N. Futaba et al.:** A black body absorber from vertically aligned single-walled carbon nanotubes. *Proceedings of the National Academy of Sciences of the United States of America* 106(15): 6044-6047 (2009).

21 **Hone, J., B. Batlogg, Z. Benes, A.T. Johnson, and J.E. Fischer:** Quantized phonon spectrum of single-wall carbon nanotubes. *Science* 289(5485): 1730-1733 (2000).

22 **Thomas, M.L., and B.S. Cohen:** A Simple Method for Vapor Dosing of Charcoal Sorbent Tubes. *American Industrial Hygiene Association Journal* 56(1): 70-73 (1995).

23 **Li, Q.L., D.X. Yuan, and Q.M. Lin:** Evaluation of multi-walled carbon nanotubes as an adsorbent for trapping volatile organic compounds from environmental samples. *Journal of Chromatography A* 1026(1-2): 283-288 (2004).

24 **Saridara, C., R. Brukh, Z. Iqbal, and S. Mitra:** Preconcentration of volatile organics on self-assembled, carbon nanotubes in a microtrap. *Analytical Chemistry* 77(4): 1183-1187 (2005).

25 **Zheng, F., D.L. Baldwin, L.S. Fifield, N.C. Anheier, C.L. Aardahl, and J.W. Grate:** Single-walled carbon nanotube paper as a sorbent for organic vapor preconcentration. *Analytical Chemistry* 78(7): 2442-2446 (2006).

CONCLUSIONS

This study was proposed to develop new sorbents in our ongoing effort to make use of our new pre-analysis technique, photothermal desorption (PTD), for VOCs. The development of new sorbents in combination with PTD has many benefits for the field of environmental and occupational health. Of significant note are the rapid analysis time for exposure assessment results and ease of use. In this study, we focused the majority of our research on two types of single-walled carbon nanotubes (SWNTs) including arc discharge (AD) and high-pressure carbon monoxide (HiPco) as potential sorbents. SWNTs were desirable due to their large specific surface area, thermal conductivity, and efficient light absorption.

In the first study, the materials were fabricated into a self-supporting form, buckypaper (BP), for easy handling as a substrate in passive air samplers. A vacuum filtration method was employed and different solvents were used for suspension and rinsing/cleaning purposes. Adsorption properties of BPs in terms of Brunauer, Emmett, and Teller (BET) surface area, pore size, and toluene adsorption capacity were characterized and compared between fabrication methods. HiPco BP had the highest BET surface area (649 m^2/g) with the smallest mean pore diameter (7.7 nm) and the greatest adsorption capacity (106 mg/g), followed by methanol-cleaned, acetone-cleaned, and non-cleaned AD BPs.

In the second study, different heat treatment conditions were examined to determine the specific conditions that improve the adsorption properties and keep the integrity of the BP unaltered for each type of BPs. Heat treatments at 300 °C for 90 minutes and 300 °C for 30 minutes were selected for acetone-cleaned AD BP and HiPco BP, respectively, based on the obtained high BET surface area (970 and 933 m^2/g, respectively) and physical integrity of the BP sorbents. After preliminary heat treatment, methanol-cleaned AD BP was eliminated for further study due to its significant change in shape.

For the last study, the heat treated, acetone-cleaned AD BP and HiPco BP were tested for PTD using 864 μg vaporized toluene preloaded on the materials. Acetone-cleaned AD BPs had the higher desorption, ranging from 0.016 to 0.431 % (0.139 to 3.721 μg), when irradiated with single visible light pulses at all energy levels examined (1.84 to 7.37 J). The proportion of desorbed analyte can be used to estimate the air concentration where the sample was collected. From this study it was determined that the heat treated acetone-cleaned AD BP is a viable sorbent for efficient VOC sampling and analysis with PTD.

Quantification/qualification of the desorbed analytes can be achieved using a variety of analytical equipment such as a photoionization detector (PID) or portable GC. When used in the field, the PTD system will yield greater sensitivity compared to direct reading instruments (DRIs). With the PTD system, exposure levels can be checked whenever needed since only a small portion of an analyte will be released, preserving the rest for later analysis. The faster turn-around-time of the analytical results and reusable BP sorbents will help protect workers' health at earlier stages of exposure. Also this new

technique can be extended to environmental sampling which requires markedly enhanced sensitivity. If more detailed analysis is needed, the BP sorbents can be further analyzed in the laboratory.

This study does have limitations however, and further experiments using more sophisticated, precise PTD set-up should be established for better control of the PTD system. Parameters which affect the desorbed amount of the analyte such as the distance from the irradiation unit to the chamber, the set of the specific light energy (voltage), and repeatability of the light pulses delivered should be further investigated and addressed in the future. As expected, desorption was proportional to the light energy levels. However, to find the most appropriate way to deliver light energy and to examine the effect of frequency on desorption, desorption through multiple pulses should be explored further. Temperature measurements of the BP sorbent during irradiation would be another set of critical data to obtain. In this study, the only VOC used was toluene, other VOCs should be introduced to the PTD system for comparison and analysis. The adsorption and PTD desorption will be affected by the polarity of VOCs, therefore it would be necessary to functionalize the BP sorbents which are nonpolar in nature.

In addition, we would like to examine other adsorbents in particular those obtained through hydrothermal carbonization (HTC) process. The HTC process is a thermochemical conversion of biomass (e.g., glucose, xylose, starch, etc.) into a carbonaceous solid. A self-supporting form, a monolith, can be directly synthesized by adding graphene oxide to the HTC process. Nanofibers can be synthesized through the HTC process as well, and fabricated into a self-supporting form through the vacuum filtration method. The HTC process is considered an alternative to the current synthesis

methods for carbonaceous materials due to its simple, inexpensive process, producing relatively less toxic materials, and the availability of an enormous variety of fabrication methods depending on their applications (e.g., adsorbents, energy storage, etc.).

GENERAL LIST OF REFERENCES

1 **OSHA:** "Training and Reference Materials Library- Industrial Hygiene." [Online] Available at https://www.osha.gov/dte/library/materials_library.html

2 *Fundamentals Of Industrial Hygiene*: NSC PRESS, 2002.

3 **Goldstein, A.H., and I.E. Galbally:** Known and unexplored organic constituents in the earth's atmosphere. *Environmental Science and Technology* 41(5): 1514-1521 (2007).

4 **EPA:** "Technial Overview of Volatile Organic Compounds." [Online] Available at https://www.epa.gov/indoor-air-quality-iaq/technical-overview-volatile-organic-compounds#3 (Accessed June 6th, 2016

5 29 CFR 1917.28 App A - Health Hazard Definitions, " *OSHA*.

6 **EPA:** "Volatile Organic Compounds' Impact on Indoor Air Quality." [Online] Available at https://www.epa.gov/indoor-air-quality-iaq/volatile-organic-compounds-impact-indoor-air-quality#Health_Effects

7 **Health, M.D.o.:** "Volatile Organic Compounds in Your Home." [Online] Available at http://www.health.state.mn.us/divs/eh/indoorair/voc/

8 **Purvis, K.L., I.O. Jumba, S. Wandiga, J. Zhang, and D.M. Kammen:** Worker exposure and health risks from volatile organic compounds utilized in the paint manufacturing industry of Kenya. *Applied Occupational and Environmental Hygiene* 16(11): 1035-1042 (2001).

9 **He, Z., G. Li, J. Chen, Y. Huang, T. An, and C. Zhang:** Pollution characteristics and health risk assessment of volatile organic compounds emitted from different plastic solid waste recycling workshops. *Environment International* 77: 85-94 (2015).

10 **Snyder, R., G. Witz, and B.D. Goldstein:** The toxicology of benzene. *Environmental Health Perspectives* 100: 293-306 (1993).

11 **Aksoy, M., and S. Erdem:** Follow up study on the mortality and the development of leukemia in 44 pancytopenic patients with chronic exposure to benzene. *Blood* 52(2): 285-292 (1978).

12 **Sarma, S.N., Y.J. Kim, and J.C. Ryu:** Differential gene expression profiles of human leukemia cell lines exposed to benzene and its metabolites. *Environmental Toxicology and Pharmacology* 32(2): 285-295 (2011).

13 **Donald, J.M., K. Hooper, and C. Hopenhayn-Rich:** Reproductive and development toxicity of toluene: A review. *Environmental Health Perspectives* 94: 237-244 (1991).

14 **Jones, H.E., and R.L. Balster:** Neurobehavioral consequences of intermittent prenatal exposure to high concentrations of toluene. *Neurotoxicology and Teratology* 19(4): 305-313 (1997).

15 **Rosenberg, N.L., B.K. Kleinschmidt-DeMasters, K.A. Davis, J.N. Dreisbach, J.T. Hormes, and C.M. Filley:** Toluene abuse causes diffuse central nervous system white matter changes. *Annals of Neurology* 23(6): 611-614 (1988).

16 **Shih-Wei, T., and S.S. Que Hee:** A new passive sampler for regulated workplace ketones. *AIHAJ* 61(6): 808-814 (2000).

17 **Berlin, A., R.H. Brown, K. Leichnitz, B. Miller, K.J. Saunders, and B. Striefler:** Diffusive Sampling—An Alternative Approach. *Applied Industrial Hygiene* 3(2): R-2-R-6 (1988).

18 **Ramachandran, G.:** *Occupational Exposure Assessment for Air Contaminants*: CRC Press Taylor & Francis Group, 2005.

19 **OSHA:** "OHSA Technical Manual - Section II - Chapter 1 - Personal Sampling for Air Contaminants." [Online] Available at https://www.osha.gov/dts/osta/otm/otm_ii/otm_ii_1.html#appendix_II_3

20 **S. J. Gregg, K.S.W.S.:** *Adsorption, Surface Area and Posority*: ACADEMIC PRESS INC. (LONDON) LTD, 1981.

21 **IUPAC:** Manual of Symbols and Terminology, Appendix 2, Part 1. *Pure Appl. Chem*. 31: 578 (1972).

22 **Webb, P.A.:** "Introduction to Chemical Adsorption Anlaytical Techniques and their Applications to Catalysis": Micromeritics Instrument Corp., 2003.

23 **Foo, K.Y., and B.H. Hameed:** Insights into the modeling of adsorption isotherm systems. *Chemical Engineering Journal* 156(1): 2-10 (2010).

24 **Balbuena, P.B., and K.E. Gubbins:** Theoretical interpretation of adsorption behavior of simple fluids in slit pores. *Langmuir* 9(7): 1801-1814 (1993).

25 **Rouquerol, J., F. Rouquerol, P. Llewellyn, G. Maurin, and K.S.W. Sing:** *Adsorption by Powders and Porous Solids: Principles, Methodology and Applications: Second Edition*, 2013.

26 **Yang, C.M., K. Kaneko, M. Yudasaka, and S. Iijima:** Effect of Purification on Pore Structure of HiPco Single-Walled Carbon Nanotube Aggregates. *Nano Letters* 2(4): 385-388 (2002).

27 **Pelekani, C., and V.L. Snoeyink:** Competitive adsorption between atrazine and methylene blue on activated carbon: The importance of pore size distribution. *Carbon* 38(10): 1423-1436 (2000).

28 **Long, C., A. Li, H. Wu, F. Liu, and Q. Zhang:** Polanyi-based models for the adsorption of naphthalene from aqueous solutions onto nonpolar polymeric adsorbents. *Journal of Colloid and Interface Science* 319(1): 12-18 (2008).

29 **Kim, K.J., and H.G. Ahn:** The effect of pore structure of zeolite on the adsorption of VOCs and their desorption properties by microwave heating. *Microporous and Mesoporous Materials* 152: 78-83 (2012).

30 **Fabrizi, G., M. Fioretti, and L. Mainero Rocca:** Occupational exposure to complex mixtures of volatile organic compounds in ambient air: Desorption from activated charcoal using accelerated solvent extraction can replace carbon disulfide? *Analytical and Bioanalytical Chemistry* 405(2-3): 961-976 (2013).

31 **NIOSH:** "Manual of Analytical Methods (NMAM), AROMATIC HYDROCARBONS: METHOD 1501." 2003.

32 **NIOSH:** "Manual of Analytical Methods (NMAM), METHYLENE CHLORIDE: METHOD 1005." 1998.

33 **NIOSH:** "Manual of Analytical Methods (NMAM), HALOGENATED HYDROCARBONS: METHOD 1003." 2003.

34 **NIOSH:** "Manual of Analytical Methods (NMAM), ETHYL ACETATE: METHOD 1457." 1994.

35 **Center for Environmental Research Information, O.R.a.D., U.S. EPA:** "Compendium Method TO-17: Determination of Volatile Oragnic Compounds in Ambient Air Using Active Sampling Onto Sorbent Tubes." U.S. EPA: U.S. EPA.

36 **Chien, Y.C., L.J. Wu, and J.H. Lwo:** The application of diffusive sampling combined with thermal desorption in occupational exposure monitoring - Field evaluation. *Applied Occupational and Environmental Hygiene* 18(5): 368-373 (2003).

37 **ASTDR:** "Toxicological Profile for Carbon Disulfide." 1996.

38 **Batterman, S., T. Metts, P. Kalliokoski, and E. Barnett:** Low-flow active and passive sampling of VOCs using thermal desorption tubes: Theory and application at an offset printing facility. *Journal of Environmental Monitoring* 4(3): 361-370 (2002).

39 **MAKERS international, I.:** "UNITY-xr." [Online] Available at https://www.markes.com/Products/Instrumentation/UNITY.aspx

40 **MAKERS international, I.:** "TD100-xr." [Online] Available at https://www.markes.com/Products/Instrumentation/TD-100.aspx

41 **Giergielewicz-Mozajska, H., L. Dabrowski, and J. Namieśnik:** Accelerated solvent extraction (ASE) in the analysis of environmental solid samples - Some aspects of theory and practice. *Critical Reviews in Analytical Chemistry* 31(3): 149-165 (2001).

42 **Koziel, J.A., and J. Pawliszyn:** Air Sampling and Analysis of Volatile Organic Compounds with Solid Phase Microextraction. *Journal of the Air & Waste Management Association* 51(2): 173-184 (2001).

43 **Harper, M.:** Sorbent trapping of volatile organic compounds from air. *Journal of Chromatography A* 885(1-2): 129-151 (2000).

44 **Floyd, E.L., K. Sapag, J. Oh, and C.T. Lungu:** Photothermal desorption of single-walled carbon nanotubes and coconut shell-activated carbons using a continuous light source for application in air sampling. *Annals of Occupational Hygiene* 58(7): 877-888 (2014).

45 **Floyd, E.L.:** Photothermal desorption of toluene from single walled carbon nanotube and activated carbon sorbents, pp. 152. Ann Arbor: The University of Alabama at Birmingham, 2013.

46 **Iijima, S.:** Helical microtubules of graphitic carbon. *Nature* 354(6348): 56-58 (1991).

47 **M. M. A. Rafique, J.I.:** Production of Carbon Nanotubes by Different Routes - A Review. *J. of Encapsulation and Adsorption Sciences* (1): 29-34 (2011).

48 **Dai, H.:** Carbon nanotubes: Synthesis, integration, and properties. *Accounts of Chemical Research* 35(12): 1035-1044 (2002).

49 **Valcárcel, M., B.M. Simonet, S. Cárdenas, and B. Suárez:** Present and future applications of carbon nanotubes to analytical science. *Analytical and Bioanalytical Chemistry* 382(8): 1783-1790 (2005).

50 **Javey, A., M. Shim, and H. Dai:** Electrical properties and devices of large-diameter single-walled carbon nanotubes. *Applied Physics Letters* 80(6): 1064-1066 (2002).

51 **Dresselhaus, M.S.:** Nanotubes: Burn and interrogate. *Science* 292(5517): 650-651 (2001).

52 **Dervishi, E., Z. Li, Y. Xu, V. Saini, A.R. Biris, D. Lupu et al.:** Carbon nanotubes: Synthesis, properties, and applications. *Particulate Science and Technology* 27(2): 107-125 (2009).

53 **Mizuno, K., J. Ishii, H. Kishida, Y. Hayamizu, S. Yasuda, D.N. Futaba et al.:** A black body absorber from vertically aligned single-walled carbon nanotubes. *Proceedings of the National Academy of Sciences of the United States of America* 106(15): 6044-6047 (2009).

54 **Pop, E., D. Mann, Q. Wang, K. Goodson, and H. Dai:** Thermal conductance of an individual single-wall carbon nanotube above room temperature. *Nano Letters* 6(1): 96-100 (2006).

55 **Volkov, A.N., and L.V. Zhigilei:** Heat conduction in carbon nanotube materials: Strong effect of intrinsic thermal conductivity of carbon nanotubes. *Applied Physics Letters* 101(4)(2012).

56 **Li, Q., C. Liu, X. Wang, and S. Fan:** Measuring the thermal conductivity of individual carbon nanotubes by the Raman shift method. *Nanotechnology* 20(14)(2009).

57 **Eswaramoorthy, M., R. Sen, and C.N.R. Rao:** A study of micropores in single-walled carbon nanotubes by the adsorption of gases and vapors. *Chemical Physics Letters* 304(3-4): 207-210 (1999).

58 **Bacsa, R.R., C. Laurent, A. Peigney, W.S. Bacsa, T. Vaugien, and A. Rousset:** High specific surface area carbon nanotubes from catalytic chemical vapor deposition process. *Chemical Physics Letters* 323(5-6): 566-571 (2000).

59 **Cinke, M., J. Li, B. Chen, A. Cassell, L. Delzeit, J. Han et al.:** Pore structure of raw and purified HiPco single-walled carbon nanotubes. *Chemical Physics Letters* 365(1-2): 69-74 (2002).

60 **Karthikeyan, S., P. Mahalingam, and M. Karthik:** Large scale synthesis of carbon nanotubes. *E-Journal of Chemistry* 6(1): 1-12 (2009).

61 **Bronikowski, M.J., P.A. Willis, D.T. Colbert, K.A. Smith, and R.E. Smalley:** Gas-phase production of carbon single-walled nanotubes from carbon monoxide via the HiPco process: A parametric study. *Journal of Vacuum Science & Technology A* 19(4): 1800-1805 (2001).

62 **Ruoff, R.S., D. Qian, and W.K. Liu:** Mechanical properties of carbon nanotubes: Theoretical predictions and experimental measurements. *Comptes Rendus Physique* 4(9): 993-1008 (2003).

63 **Liew, K.M., J.W. Yan, Y.Z. Sun, and L.H. He:** Investigation of temperature effect on the mechanical properties of single-walled carbon nanotubes. *Composite Structures* 93(9): 2208-2212 (2011).

64 **Walters, D.A., L.M. Ericson, M.J. Casavant, J. Liu, D.T. Colbert, K.A. Smith et al.:** Elastic strain of freely suspended single-wall carbon nanotube ropes. *Applied Physics Letters* 74(25): 3803-3805 (1999).

65 **Li, F., H.M. Cheng, S. Bai, G. Su, and M.S. Dresselhaus:** Tensile strength of single-walled carbon nanotubes directly measured from their macroscopic ropes. *Applied Physics Letters* 77(20): 3161-3163 (2000).

66 **Pan, Z.W., S.S. Xie, L. Lu, B.H. Chang, L.F. Sun, W.Y. Zhou et al.:** Tensile tests of ropes of very long aligned multiwall carbon nanotubes. *Applied Physics Letters* 74(21): 3152-3154 (1999).

67 **Yu, M.F., O. Lourie, M.J. Dyer, K. Moloni, T.F. Kelly, and R.S. Ruoff:** Strength and breaking mechanism of multiwalled carbon nanotubes under tensile load. *Science* 287(5453): 637-640 (2000).

68 **Krishnan, A., E. Dujardin, T.W. Ebbesen, P.N. Yianilos, and M.M.J. Treacy:** Young's modulus of single-walled nanotubes. *Physical Review B - Condensed Matter and Materials Physics* 58(20): 14013-14019 (1998).

69 **Serway, R.A.a.J., J. W. Jr.:** *Physics for Scientists and Engineers with Modern Physics*: Thomson Higher Education, 2008.

70 **Theocharous, E., R. Deshpande, A.C. Dillon, and J. Lehman:** Evaluation of a pyroelectric detector with a carbon multiwalled nanotube black coating in the infrared. *Applied Optics* 45(6): 1093-1097 (2006).

71 **Cao, A., X. Zhang, C. Xu, B. Wei, and D. Wu:** Tandem structure of aligned carbon nanotubes on Au and its solar thermal absorption. *Solar Energy Materials and Solar Cells* 70(4): 481-486 (2002).

72 **Wang, X.J., J.D. Flicker, B.J. Lee, W.J. Ready, and Z.M. Zhang:** Visible and near-infrared radiative properties of vertically aligned multi-walled carbon nanotubes. *Nanotechnology* 20(21)(2009).

73 **Wang, S., Z. Bai, G. Yan, H. Zhang, J. Wang, W. Yu et al.:** The enhancement of photo-thermo-electric conversion in tilted Bi2Sr2Co2Oy thin films through coating a layer of single-wall carbon nanotubes light absorber. *Optics Express* 21(15): 18336-18343 (2013).

74 **Endo, M., T. Hayashi, Y.A. Kim, and H. Muramatsu:** Development and application of carbon nanotubes. *Japanese Journal of Applied Physics, Part 1: Regular Papers and Short Notes and Review Papers* 45(6 A): 4883-4892 (2006).

75 **LaBrosse, M.R., W. Shi, and J. Karl Johnson:** Adsorption of gases in carbon nanotubes: Are defect interstitial sites important? *Langmuir* 24(17): 9430-9439 (2008).

76 **Liu, C., Y.Y. Fan, M. Liu, H.T. Cong, H.M. Cheng, and M.S. Dresselhaus:** Hydrogen storage in single-walled carbon nanotubes at room temperature. *Science* 286(5442): 1127-1129 (1999).

77 **Ye, Y., C.C. Ahn, C. Witham, B. Fultz, J. Liu, A.G. Rinzler et al.:** Hydrogen adsorption and cohesive energy of single-walled carbon nanotubes. *Applied Physics Letters* 74(16): 2307-2309 (1999).

78 **Muris, M., N. Dufau, M. Bienfait, N. Dupont-Pavlovsky, Y. Grillet, and J.P. Palmari:** Methane and krypton adsorption on single-walled carbon nanotubes. *Langmuir* 16(17): 7019-7022 (2000).

79 **Ulbricht, H., J. Kriebel, G. Moos, and T. Hertel:** Desorption kinetics and interaction of Xe with single-wall carbons nanotube bundles. *Chemical Physics Letters* 363(3-4): 252-260 (2002).

80 **Babaa, M.R., N. Dupont-Pavlovsky, E. McRae, and K. Masenelli-Varlot:** Physical adsorption of carbon tetrachloride on as-produced and on mechanically opened single walled carbon nanotubes. *Carbon* 42(8-9): 1549-1554 (2004).

81 **Bienfait, M., P. Zeppenfeld, N. Dupont-Pavlovsky, M. Muris, M. Johnson, T. Wilson et al.:** Thermodynamics and structure of hydrogen, methane, argon, oxygen and carbon dioxide adsorbed on single wall carbon nanotube bundles. *Physica B: Condensed Matter* 350(1-3 SUPPL. 1): e423-e426 (2004).

82 **Muris, M., N. Dupont-Pavlovsky, M. Bienfait, and P. Zeppenfeld:** Where are the molecules adsorbed on single-walled nanotubes? *Surface Science* 492(1-2): 67-74 (2001).

83 **Talapatra, S., A.Z. Zambano, S.E. Weber, and A.D. Migone:** Gases do not adsorb on the interstitial channels of closed-ended single-walled carbon nanotube bundles. *Physical Review Letters* 85(1): 138-141 (2000).

84 **Teizer, W., R.B. Hallock, E. Dujardin, and T.W. Ebbesen:** 4He desorption from single wall carbon nanotube bundles: A one-dimensional adsorbate. *Physical Review Letters* 82(26 I): 5305-5308 (1999).

85 **Shi, W., and J.K. Johnson:** Gas adsorption on heterogeneous single-walled carbon nanotube bundles. *Physical Review Letters* 91(1): 015504/015501-015504/015504 (2003).

86 **Hou, P.X., C. Liu, and H.M. Cheng:** Purification of carbon nanotubes. *Carbon* 46(15): 2003-2025 (2008).

87 **Babaa, M.R., I. Stepanek, K. Masenelli-Varlot, N. Dupont-Pavlovsky, E. McRae, and P. Bernier:** Opening of single-walled carbon nanotubes: Evidence given by krypton and xenon adsorption. *Surface Science* 531(1): 86-92 (2003).

88 **Di, J., D. Hu, H. Chen, Z. Yong, M. Chen, Z. Feng et al.:** Ultrastrong, foldable, and highly conductive carbon nanotube film. *ACS Nano* 6(6): 5457-5464 (2012).

89 **Shi, Z., X. Chen, X. Wang, T. Zhang, and J. Jin:** Fabrication of superstrong ultrathin free-standing single-walled carbon nanotube films via a wet process. *Advanced Functional Materials* 21(22): 4358-4363 (2011).

90 **Zheng, F., D.L. Baldwin, L.S. Fifield, N.C. Anheier, C.L. Aardahl, and J.W. Grate:** Single-walled carbon nanotube paper as a sorbent for organic vapor preconcentration. *Analytical Chemistry* 78(7): 2442-2446 (2006).

91 **Saridara, C., R. Brukh, Z. Iqbal, and S. Mitra:** Preconcentration of volatile organics on self-assembled, carbon nanotubes in a microtrap. *Analytical Chemistry* 77(4): 1183-1187 (2005).

92 **Hussain, C.M., C. Saridara, and S. Mitra:** Microtrapping characteristics of single and multi-walled carbon nanotubes. *Journal of Chromatography A* 1185(2): 161-166 (2008).